ROBUST VIRTUAL ELEMENT METHODS FOR COUPLED STRESS-ASSISTED DIFFUSION PROBLEMS*

REKHA KHOT[†], ANDRÉS E. RUBIANO[‡], AND RICARDO RUIZ-BAIER[§]

Abstract. This paper aims first to perform robust continuous analysis of a mixed nonlinear formulation for stress-assisted diffusion of a solute that interacts with an elastic material, and second to propose and analyse a virtual element formulation of the model problem. The two-way coupling mechanisms between the Herrmann formulation for linear elasticity and the reaction-diffusion equation (written in mixed form) consist of diffusion-induced active stress and stress-dependent diffusion. The two sub-problems are analysed using the extended Babuška–Brezzi–Braess theory for perturbed saddle-point problems. The well-posedness of the nonlinearly coupled system is established using a Banach fixed-point strategy under the smallness assumption on data. The virtual element formulations for the uncoupled sub-problems are proven uniquely solvable by a fixed-point argument in conjunction with appropriate projection operators. We derive the a priori error estimates, and test the accuracy and performance of the proposed method through computational simulations.

Key words. Virtual element methods, stress-assisted diffusion, diffusion-induced stress, perturbed saddle-point problems, fixed-point operators.

AMS subject classifications. 65N30, 65N12, 65N15, 74F25.

1. Introduction.

The process of diffusion within solid matter can result in the creation of mechanical stresses within the solid material, commonly referred to as chemical or diffusion-induced stresses. This phenomenon highlights a reciprocal relationship between chemical and mechanical driving forces, both of which play a key role in either facilitating or hindering the diffusion process. Stress-assisted diffusion for common materials has been introduced as a general formalism in [35, 34]. Important examples include Lithium-ion battery cells, silicon rubber and hydrogen diffusion, polymer-based coatings, semiconductor fabrication, oxidation of silicon nanostructures, and enhancing of conductivity properties in soft living tissue. In these processes, heterogeneity (and possibly also anisotropy) of stress localisation affects the patterns of diffusion. Our contribution addresses one of the simplest models for such an interaction, incorporating stress-dependency directly in the diffusion coefficient for a given solute, and assuming that in the absence of stress one recovers Fickian diffusion (see, e.g., [11, 37]). We consider the regime of linear elastostatics and assume that the total Cauchy stress is also due to a (possibly nonlinear) diffusion-induced isotropic stress. On the other hand, the diffusion coefficient in the reaction-diffusion equation governing the distribution of a solute is taken as a nonlinear function of the Cauchy stress. The well-posedness of primal formulations of the coupled problem has been studied in, e.g., [25, 26].

Some of the materials mentioned above are nearly incompressible, which is why we opt for a mixed formulation of the elastostatics in terms of displacement and Herrmann pressure [6, 21], which allows us to have stability robustly with respect to the Lamé parameter λ that goes to infinity when the Poisson ration approaches $\frac{1}{2}$. Robustness with respect to the Lamé parameter μ can be obtained from appropriate scaling of the inf-sup condition for the divergence operator, as done in, e.g., [22, 31]. Robustness with respect to the Lamé parameters is also required for the reaction-diffusion sub-problem, which is a priori not trivial since the diffusion coefficient depends on the Cauchy stress and in turn on the Lamé coefficients. Similarly to the diffusion-assisted elasticity, the stress-assisted reaction-diffusion problem is written as a perturbed saddle-point problem, and robustness is sought also with respect to the uniform bounds of the stress-assisted diffusion and of the reaction parameter. We therefore work with parameter-weighted norms and use the perturbed saddle-point theory from [7, 8]. The continuous analysis is then adequately adapted to the discrete case, here using virtual element methods (VEMs).

There has been quite a few works on the mixed finite element methods for the stress-assisted diffusion problems, see e.g., [15, 16, 17, 18, 19]. The standard finite element methods (FEM) are well-adapted for many realistic models, but from the past decade, polygonal methods are fast emerging due to their capabilities for mesh flexibility and a common framework for higher-degrees and for higher-dimensions. The VEM

*Updated: January 18, 2024.

Funding: This work has been partially supported by the Australian Research Council through the Future Fellowship grant FT220100496 and Discovery Project grant DP22010316.

[†]School of Mathematics, Monash University, 9 Rainforest Walk, Melbourne, VIC 3800, Australia. Present address: Inria 75012, Paris, France (rekha.khot@inria.fr).

[‡]School of Mathematics, Monash University, 9 Rainforest Walk, Melbourne, VIC 3800, Australia (Andres.RubianoMartinez@monash.edu).

[§]School of Mathematics, Monash University, 9 Rainforest Walk, Melbourne, VIC 3800, Australia; and Universidad Adventista de Chile, Casilla 7-D, Chillán, Chile (Ricardo.RuizBaier@monash.edu).

first introduced in [2] is one of the popular polygonal methods, which can be viewed as the generalisation of FEM. The VEM setting takes into consideration the typical terminologies in FEM like conforming, nonconforming, or mixed methods, and that allows to modify the well-developed tools from FEM in somewhat similar manner. The local VE spaces are defined as a set of solutions to problem-dependent partial differential equations combined with boundary conditions based on the underline nature of the method we are interested in (e.g., conforming or nonconforming). Of course a leap from triangular/rectangular elements to fairly general polygonal-shaped elements forces to include locally the non-polynomial shape functions in addition to polynomials. But VEM stands different from the other methods in a sense that it does not require to compute explicitly the possibly complex shape functions and the complete analysis can be performed through degrees of freedom (DoFs) of VE functions and their appropriate projections from the local discrete space to the polynomial subspace. The vast literature is available on VEM and we name just a few here [10, 3, 4, 28] which are relevant to the model problem in this paper. VEM is still not explored much for coupled problems, see [1] for the Navier–Stokes coupled with the heat equation, and this paper is the first one on the coupled stress-assisted diffusion problems to the best of authors' knowledge. We restrict VE spaces and analysis to 2D for simplicity, but extension to 3D is possible. For example, we refer to [5] and [12] for Stokes and mixed Darcy problems in three dimensions.

Plan of the paper. The contents of this paper have been organised in the following manner. The remainder of this introductory section contains preliminary notational conventions and definitions of useful functional spaces. Section 2 presents the precise definition of the coupled stress-assisted diffusion model we will address, along with the derivation of its weak formulation in the form of two coupled perturbed saddle-point problems. The unique solvability of the model problem is studied in Section 3, using the Banach fixed-point approach. Section 4 is devoted to designing a family of VEMs for the system under consideration, defining virtual spaces, and recalling appropriate projection operators. In Subsection 4.3 we use an abstract result for discrete perturbed saddle-point problems and again the fixed-point theory, to show that the discrete problem is well-posed. The a priori error analysis for the VE method is carried out in Section 5. Finally, the convergence rates and robustness of the proposed formulation are tested numerically in Section 6.

Recurrent notation and Sobolev spaces. Let D be a polygonal Lipschitz bounded domain of $\mathbb{R}^2$ with boundary ∂D. In this paper we apply all differential operators row-wise. Hence, given a tensor function $\boldsymbol{\sigma}: D \to \mathbb{R}^{2\times 2}$ and a vector field $\boldsymbol{u}: D \to \mathbb{R}^2$, we set the tensor divergence $\mathbf{div}\,\boldsymbol{\sigma}: D \to \mathbb{R}^2$, the vector gradient $\boldsymbol{\nabla u}: D \to \mathbb{R}^{2\times 2}$, and the symmetric gradient $\boldsymbol{\varepsilon}(\boldsymbol{u}): D \to \mathbb{R}^{2\times 2}$ as $(\mathbf{div}\,\boldsymbol{\sigma})_i := \sum_j \partial_j \sigma_{ij}$, $(\boldsymbol{\nabla u})_{ij} := \partial_j u_i$, and $\boldsymbol{\varepsilon}(\boldsymbol{u}) := \frac{1}{2}\left[\boldsymbol{\nabla u} + (\boldsymbol{\nabla u})^{\mathtt{t}}\right]$. The component-wise inner product of two matrices $\boldsymbol{\sigma}, \boldsymbol{\tau} \in \mathbb{R}^{2\times 2}$ is defined by $\boldsymbol{\sigma} : \boldsymbol{\tau} := \sum_{i,j} \sigma_{ij}\tau_{ij}$. For $s \geq 0$, we denote the usual Hilbertian Sobolev space of scalar functions with domain D by $H^s(D)$, and denote their vector and tensor counterparts as $\mathbf{H}^s(D)$ and $\mathbb{H}^s(D)$, respectively. The norm of $H^s(D)$ is denoted $\|\cdot\|_{s,D}$ and the corresponding semi-norm $|\cdot|_{s,D}$. We also use the convention $H^0(D) := L^2(D)$ and the notation $L^2_0(D)$ when the zero mean value condition is imposed, and $(\cdot,\cdot)_D$ to denote the inner product in $L^2(D)$ (similarly for the vector and tensor counterparts). The space of vectors in $\mathbf{L}^2(D)$ with divergence in $L^2(D)$ is denoted $\mathbf{H}(\mathrm{div}, D)$ and it is a Hilbert space equipped with the corresponding graph norm $\|\boldsymbol{\zeta}\|^2_{\mathrm{div},D} := \|\boldsymbol{\zeta}\|^2_{0,D} + \|\mathrm{div}\,\boldsymbol{\zeta}\|^2_{0,D}$. The same way around with rotational in $L^2(D)$ which is a Hilbert space denoted by $\mathbf{H}(\mathrm{rot}, D)$ with the natural norm $\|\boldsymbol{\zeta}\|^2_{\mathrm{rot},D} := \|\boldsymbol{\zeta}\|^2_{0,D} + \|\mathrm{rot}\,\boldsymbol{\zeta}\|^2_{0,D}$. Let $\boldsymbol{n}$ be the outward unit normal vector to ∂D. The Green Formula can be used to extend the normal trace operator $\mathbb{C}^\infty(\overline{D}) \ni \boldsymbol{\zeta} \to (\boldsymbol{\zeta}|_{\partial D}) \cdot \boldsymbol{n}$ to a linear continuous mapping $(\cdot|_{\partial D}) \cdot \boldsymbol{n} : \mathbf{H}(\mathrm{div}, D) \to H^{-\frac{1}{2}}(\partial D)$, where $H^{-\frac{1}{2}}(\partial D)$ is the dual of $H^{\frac{1}{2}}(\partial D)$ (see [14, Theorem 1.7]). Moreover, the well-known trace inequality $|\langle(\boldsymbol{\zeta}|_{\partial D}) \cdot \boldsymbol{n}, r^*\rangle_{\partial D}| \leq \|\boldsymbol{\zeta}\|_{\mathrm{div},D}\|r^*\|_{\frac{1}{2},\partial D}$ holds, where $\langle\cdot,\cdot\rangle_{\partial D}$ denotes the duality pairing between $H^{\frac{1}{2}}(\partial D)$ and $H^{-\frac{1}{2}}(\partial D)$ with respect to the inner product in $L^2(\partial D)$ and the norm in the traces space $H^{\frac{1}{2}}(\partial D)$ is defined as $\|r^*\|_{\frac{1}{2},\partial D} = \inf_{r|_{\partial D} = r^*} \|r\|_{1,\Omega}$. An analogous argument extends the notion of trace operators to subsets of ∂D.

We shall use the letter C to denote a generic positive constant independent of the mesh size h and physical constants, which might stand for different values at its different occurrences. Moreover, given any positive expressions X and Y, the notation $X \lesssim Y$ means that $X \leq CY$.

2. Governing equations.

This section introduces the model problem in detail with the required assumptions on the involved coefficients and the corresponding weak formulation at the end.

2.1. Model statement.

Let us consider a deformable body occupying the domain Ω and satisfying the balance of linear momentum in the stationary regime

$$-\,\mathbf{div}\,\boldsymbol{\sigma} = \boldsymbol{f} \qquad \text{in } \Omega, \tag{2.1}$$

where $\boldsymbol{\sigma}$ is the Cauchy stress tensor and $\boldsymbol{f}$ is a vector of external body loads. The coupling between solid deformation and a solute with concentration φ is considered using an active stress approach. Combined with Hooke's law, this gives the specification

$$\boldsymbol{\sigma} = \mathcal{C}\boldsymbol{\varepsilon}(\boldsymbol{u}) - \ell(\varphi)\mathbb{I} = 2\mu\boldsymbol{\varepsilon}(\boldsymbol{u}) + \lambda \operatorname{div} \boldsymbol{u}\, \mathbb{I} - \ell(\varphi)\mathbb{I} \qquad \text{in } \Omega, \tag{2.2}$$

where $\mathcal{C}$ is the fourth-order elasticity tensor (symmetric and positive definite), μ, λ are the Lamé parameters associated with the material properties of the solid substrate, ℓ is a nonlinear function of the solute concentration that modulates the intensity and distribution of (isotropic) active stress (also known as diffusion-induced stress), $\boldsymbol{u}$ is the displacement vector, $\boldsymbol{\varepsilon}(\boldsymbol{u})$ is the tensor of infinitesimal strains (symmetrised gradient of displacement), and $\mathbb{I}$ denotes the identity tensor in $\mathbb{R}^{2\times 2}$.

Equations (2.1)-(2.2) indicate that the solid deformation will be a response of both external loads and internal stress generation due to the coupling with the species φ. On the other hand, the solute steady transport in the solid is governed by the reaction-diffusion equation

$$\theta\varphi - \operatorname{div}(\mathbb{M}(\boldsymbol{\sigma})\nabla\varphi) = g \qquad \text{in } \Omega,$$

where g is a given net volumetric source of solute, θ is a positive model parameter, and $\mathbb{M}$ is the stress-assisted diffusion coefficient (a matrix-valued function of total stress, and assumed uniformly bounded away from zero). This term implies a two-way coupling mechanism between deformation and transport. We also consider the auxiliary variable of diffusive flux

$$\boldsymbol{\zeta} = \mathbb{M}(\boldsymbol{\sigma})\nabla\varphi \qquad \text{in } \Omega, \tag{2.3}$$

and therefore the reaction-diffusion equation reads

$$\theta\varphi - \operatorname{div} \boldsymbol{\zeta} = g \qquad \text{in } \Omega. \tag{2.4}$$

In [15, 16] the contribution of ℓ into the active stress is transferred (thanks to (2.1)) to the loading term as $\boldsymbol{f} = \boldsymbol{f}(\varphi)$. Here we maintain it as part of the volumetric stress through the Herrmann-type pressure (see [21] for the classical hydrostatic pressure formulation) which represents the *total volumetric stress* (see e.g., [24], but note that here we are including both elastic and active components)

$$\tilde{p} := -\lambda \operatorname{div} \boldsymbol{u} + \ell(\varphi) \qquad \text{in } \Omega, \tag{2.5}$$

giving that the Cauchy stress reads $\boldsymbol{\sigma} = 2\mu\boldsymbol{\varepsilon}(\boldsymbol{u}) - \tilde{p}\mathbb{I}$. This approach leads to a system similar to the total pressure formulation for linear poroelasticity in parameter-robust and conservative form (see, e.g., [7, 23]).

We adopt mixed loading boundary conditions for the coupled problem: the structure is clamped ($\boldsymbol{u} = \boldsymbol{0}$) and a given concentration $\varphi = \varphi_D$ are imposed on Γ_D, where the boundary subset $\Gamma_D \subset \partial\Omega$ is of positive surface measure; and traction and zero solute flux are prescribed ($\boldsymbol{\sigma n} = \boldsymbol{t}$ and $\boldsymbol{\zeta}\cdot\boldsymbol{n} = 0$) on $\Gamma_N := \partial\Omega\setminus\Gamma_D$.

2.2. Weak formulation. In view of the boundary conditions, we define the Hilbert spaces

$$\mathbf{H}^1_D(\Omega) := \{\boldsymbol{v} \in \mathbf{H}^1(\Omega) : \boldsymbol{v} = \boldsymbol{0} \quad \text{on } \Gamma_D\}, \qquad \mathbf{H}_N(\operatorname{div},\Omega) := \{\boldsymbol{\xi} \in \mathbf{H}(\operatorname{div},\Omega) : \boldsymbol{\xi}\cdot\boldsymbol{n} = 0 \quad \text{on } \Gamma_N\},$$

with the boundary assignment understood in the sense of traces, and consider the following weak formulation for the system composed by (2.1), (2.5), (2.3), (2.4). For given $\boldsymbol{f} \in \mathbf{L}^2(\Omega)$, $g \in L^2(\Omega)$, and $\varphi_D \in H^{\frac{1}{2}}(\Gamma_D)$, find $(\boldsymbol{u}, \tilde{p}, \boldsymbol{\zeta}, \varphi) \in \mathbf{H}^1_D(\Omega) \times L^2(\Omega) \times \mathbf{H}_N(\operatorname{div},\Omega) \times L^2(\Omega)$ such that

$$2\mu\int_\Omega \boldsymbol{\varepsilon}(\boldsymbol{u}) : \boldsymbol{\varepsilon}(\boldsymbol{v}) - \int_\Omega \tilde{p} \operatorname{div} \boldsymbol{v} = \int_\Omega \boldsymbol{f}\cdot\boldsymbol{v} \qquad \forall \boldsymbol{v} \in \mathbf{H}^1_D(\Omega), \tag{2.6a}$$

$$-\int_\Omega \tilde{q} \operatorname{div} \boldsymbol{u} - \frac{1}{\lambda}\int_\Omega \tilde{p}\tilde{q} = -\frac{1}{\lambda}\int_\Omega \ell(\varphi)\tilde{q} \qquad \forall \tilde{q} \in L^2(\Omega), \tag{2.6b}$$

$$\int_\Omega \mathbb{M}(\boldsymbol{\sigma})^{-1}\boldsymbol{\zeta}\cdot\boldsymbol{\xi} + \int_\Omega \varphi \operatorname{div} \boldsymbol{\xi} = \langle \varphi_D, \boldsymbol{\xi}\cdot\boldsymbol{n}\rangle_{\Gamma_D} \qquad \forall \boldsymbol{\xi} \in \mathbf{H}_N(\operatorname{div},\Omega), \tag{2.6c}$$

$$\int_\Omega \psi \operatorname{div} \boldsymbol{\zeta} - \theta\int_\Omega \varphi\psi = -\int_\Omega g\psi \qquad \forall \psi \in L^2(\Omega). \tag{2.6d}$$

This formulation (mixed for the nonlinear reaction-diffusion part and mixed for the active linear elasticity part) results simply multiplying by test functions and integrating by parts the terms containing the shear and volumetric parts of stress, as well as the diffusive flux.

2.3. Two uncoupled perturbed saddle-point problems. Before we investigate the unique solvability of (2.6), we will regard the nonlinear coupled problem as two separate perturbed saddle-point problems. Commonly used forms for the stress-assisted diffusion coefficient include (see, e.g., [11, 15, 20])

$$\mathbb{M}(\boldsymbol{\sigma}) = m_0\mathbb{I} + m_1\boldsymbol{\sigma} + m_2\boldsymbol{\sigma}^2, \quad \mathbb{M}(\boldsymbol{\sigma}) = m_0\exp(-m_1\operatorname{tr}\boldsymbol{\sigma})\mathbb{I}, \quad \mathbb{M}(\boldsymbol{\sigma}) = m_0\exp(-m_1\boldsymbol{\sigma}^{m_2}),$$

where $m_0, m_1, m_2 \in \mathbb{R}$ are model parameters, with $m_0 > 0$. On the other hand, a typical form of the active stress include the Hill-type function (i.e., with a modulation saturating at high concentration values see, e.g., [27, 29, 30]) or a scaling of the given concentration (see [33]), defined as

$$\ell(\vartheta) = K_0 + \frac{\vartheta^n}{K_1 + \vartheta^n}, \quad \ell(\vartheta) = K_0\vartheta,$$

where K_0, K_1 and n (Hill coefficient) are model parameters. From now on, the stress-assisted diffusion will be written explicitly as a function of the infinitesimal strain and of the total volumetric stress $\mathbb{M}(\boldsymbol{\varepsilon}(\boldsymbol{w}), \tilde{r})$. It is assumed that $\mathbb{M}(\cdot,\cdot)$ is symmetric, positive semi-definite and uniformly bounded in $\mathbb{L}^\infty(\Omega)$, likewise for $\mathbb{M}^{-1}(\cdot,\cdot)$. More explicitly, there exists a constant M such that $0 < \frac{1}{M} \leq M$ and

$$\mathbb{M}^{-1}(\boldsymbol{\varepsilon}(\boldsymbol{w}), \tilde{r}) \in \mathbb{L}^\infty(\Omega) \qquad \forall \boldsymbol{w} \in \mathbf{H}^1(\Omega), \tilde{r} \in L^2(\Omega), \tag{2.7a}$$

$$\frac{1}{M}\boldsymbol{x}\cdot\boldsymbol{x} \leq \boldsymbol{x}\cdot[\mathbb{M}^{-1}(\boldsymbol{\varepsilon}(\boldsymbol{w}), \tilde{r})\boldsymbol{x}] \qquad \forall \boldsymbol{x} \in \mathbb{R}^2, \tag{2.7b}$$

$$\boldsymbol{y}\cdot[\mathbb{M}^{-1}(\boldsymbol{\varepsilon}(\boldsymbol{w}), \tilde{r})\boldsymbol{x}] \leq M\boldsymbol{x}\cdot\boldsymbol{y} \qquad \forall \boldsymbol{x}, \boldsymbol{y} \in \mathbb{R}^2. \tag{2.7c}$$

For the active stress function $\ell(\cdot)$, we assume that $\ell : L^2(\Omega) \to L^2(\Omega)'$ and satisfies

$$\|\ell(\vartheta)\|_{0,\Omega} \lesssim \|\vartheta\|_{0,\Omega} \qquad \forall \vartheta \in L^2(\Omega). \tag{2.8}$$

Moreover, we assume that $\mathbb{M}^{-1}(\cdot,\cdot)$ and $\ell(\cdot)$ are Lipschitz continuous, i.e., for all $\boldsymbol{\tau}_1, \boldsymbol{\tau}_2 \in \mathbb{L}^2(\Omega)$ and $\tilde{r}_1, \tilde{r}_2, \vartheta_1, \vartheta_2 \in L^2(\Omega)$ there exist positive constants $L_{\mathbb{M}}$ and L_ℓ that satisfy the following bounds

$$\|\mathbb{M}^{-1}(\boldsymbol{\tau}_1, \tilde{r}_1) - \mathbb{M}^{-1}(\boldsymbol{\tau}_2, \tilde{r}_2)\|_{\infty,\Omega} \leq L_{\mathbb{M}}\|(\boldsymbol{\tau}_1, \tilde{r}_1) - (\boldsymbol{\tau}_2, \tilde{r}_2)\|_{\mathbb{L}^2(\Omega)\times L^2(\Omega)}, \tag{2.9a}$$

$$\|\ell(\vartheta_1) - \ell(\vartheta_2)\|_{0,\Omega} \leq L_\ell\|\vartheta_1 - \vartheta_2\|_{0,\Omega}. \tag{2.9b}$$

For a fixed vector-valued function $\boldsymbol{w} \in \mathbf{H}^1(\Omega)$ and a fixed scalar function $\tilde{r} \in L^2(\Omega)$, we define the following bilinear form $a_2^{\boldsymbol{w},\tilde{r}} : \mathbf{H}(\operatorname{div},\Omega) \times \mathbf{H}(\operatorname{div},\Omega) \to \mathbb{R}$ as

$$a_2^{\boldsymbol{w},\tilde{r}}(\boldsymbol{\zeta}, \boldsymbol{\xi}) := \int_\Omega \mathbb{M}^{-1}(\boldsymbol{\varepsilon}(\boldsymbol{w}), \tilde{r})\boldsymbol{\zeta}\cdot\boldsymbol{\xi} \qquad \forall \boldsymbol{\zeta}, \boldsymbol{\xi} \in \mathbf{H}(\operatorname{div},\Omega).$$

In addition, for a fixed scalar function $\vartheta \in L^2(\Omega)$, we define the linear functional $G_1^\vartheta : L^2(\Omega) \to \mathbb{R}$ as

$$G_1^\vartheta(\tilde{q}) := -\frac{1}{\lambda}\int_\Omega \ell(\vartheta)\tilde{q} \qquad \forall \tilde{q} \in L^2(\Omega).$$

Then set the bilinear forms $a_1 : \mathbf{H}^1(\Omega)\times\mathbf{H}^1(\Omega) \to \mathbb{R}$, $b_1 : \mathbf{H}^1(\Omega)\times L^2(\Omega) \to \mathbb{R}$, $c_1, c_2 : L^2(\Omega)\times L^2(\Omega) \to \mathbb{R}$, $b_2 : \mathbf{H}(\operatorname{div},\Omega)\times L^2(\Omega) \to \mathbb{R}$, and linear functionals $F_1 : \mathbf{H}^1(\Omega) \to \mathbb{R}$, $F_2 : \mathbf{H}(\operatorname{div},\Omega) \to \mathbb{R}$, $G_2 : L^2(\Omega) \to \mathbb{R}$ as follows

$$a_1(\boldsymbol{u}, \boldsymbol{v}) := 2\mu\int_\Omega \boldsymbol{\varepsilon}(\boldsymbol{u}) : \boldsymbol{\varepsilon}(\boldsymbol{v}), \quad b_1(\boldsymbol{v}, \tilde{q}) := -\int_\Omega \tilde{q}\operatorname{div}\boldsymbol{v}, \quad c_1(\tilde{p}, \tilde{q}) := \int_\Omega \tilde{p}\tilde{q}, \quad F_1(\boldsymbol{v}) := \int_\Omega \boldsymbol{f}\cdot\boldsymbol{v},$$

$$b_2(\boldsymbol{\xi}, \psi) := \int_\Omega \psi\operatorname{div}\boldsymbol{\xi}, \quad c_2(\varphi, \psi) := \int_\Omega \varphi\psi, \quad F_2(\boldsymbol{\xi}) := \langle\varphi_D, \boldsymbol{\xi}\cdot\boldsymbol{n}\rangle_{\Gamma_D}, \quad G_2(\psi) := -\int_\Omega g\psi,$$

for all $\boldsymbol{u}, \boldsymbol{v} \in \mathbf{H}^1(\Omega)$, $\tilde{p}, \tilde{q}, \varphi, \psi \in L^2(\Omega)$, $\boldsymbol{\zeta}, \boldsymbol{\xi} \in \mathbf{H}(\operatorname{div},\Omega)$, $\varphi_D \in H^{1/2}(\Gamma_D)$.

With these building blocks we define the following system of linear elasticity: for a given $\vartheta \in L^2(\Omega)$ and $\boldsymbol{f} \in \mathbf{L}^2(\Omega)$, find $(\boldsymbol{u}, \tilde{p}) \in \mathbf{H}^1_D(\Omega)\times L^2(\Omega)$ such that

$$a_1(\boldsymbol{u}, \boldsymbol{v}) + b_1(\boldsymbol{v}, \tilde{p}) = F_1(\boldsymbol{v}) \qquad \forall \boldsymbol{v} \in \mathbf{H}^1_D(\Omega), \tag{2.10a}$$

$$b_1(\boldsymbol{u}, \tilde{q}) - \frac{1}{\lambda}c_1(\tilde{p}, \tilde{q}) = G_1^\vartheta(\tilde{q}) \qquad \forall \tilde{q} \in L^2(\Omega). \tag{2.10b}$$

We also consider the following reaction-diffusion equation in weak form: for a given $\boldsymbol{w} \in \mathbf{H}^1_D(\Omega)$, $\tilde{r} \in L^2(\Omega)$, $\varphi_D \in H^{\frac{1}{2}}(\Gamma_D)$ and $g \in L^2(\Omega)$, find $(\boldsymbol{\zeta}, \varphi) \in \mathbf{H}_N(\operatorname{div},\Omega)\times L^2(\Omega)$ such that

$$a_2^{\boldsymbol{w},\tilde{r}}(\boldsymbol{\zeta}, \boldsymbol{\xi}) + b_2(\boldsymbol{\xi}, \varphi) = F_2(\boldsymbol{\xi}) \qquad \forall \boldsymbol{\xi} \in \mathbf{H}_N(\operatorname{div},\Omega), \tag{2.11a}$$

$$b_2(\boldsymbol{\zeta}, \psi) - \theta c_2(\varphi, \psi) = G_2(\psi) \qquad \forall \psi \in L^2(\Omega). \tag{2.11b}$$

3. Well-posedness of the continuous problem. The unique solvability of the elasticity and reaction-diffusion equations will be established using the theory of saddle-point problems with penalty [8, Lemma 3]. First we state an extended version of the Babuška–Brezzi theory from [7, Theorem 2.1].

THEOREM 3.1. *Let V, Q_b be Hilbert spaces endowed with the (possibly parameter-dependent) norms $\|\cdot\|_V$ and $\|\cdot\|_{Q_b}$, let Q be a dense (with respect to the norm $\|\cdot\|_{Q_b}$) linear subspace of Q_b and three bilinear forms $a(\cdot,\cdot)$ on $V\times V$ (assumed continuous, symmetric and positive semi-definite), $b(\cdot,\cdot)$ on $V\times Q_b$ (continuous), and $c(\cdot,\cdot)$ on $Q\times Q$ (symmetric and positive semi-definite); which define the linear operators $A : V \to V'$, $B : V \to Q_b'$ and $C : Q \to Q'$, respectively. Suppose further that*

$$\|\hat{v}\|_V^2 \lesssim a(\hat{v},\hat{v}) \qquad \forall \hat{v}\in \mathrm{Ker}(B), \tag{3.1a}$$

$$\|q\|_{Q_b} \lesssim \sup_{v\in V}\frac{b(v,q)}{\|v\|_V} \qquad \forall q\in Q_b. \tag{3.1b}$$

Assume that Q is complete with respect to the norm $\|\cdot\|_Q^2 := \|\cdot\|_{Q_b}^2 + t^2|\cdot|_c^2$, where $|\cdot|_c^2 := c(\cdot,\cdot)$ is a semi-norm in Q. Let $t\in[0,1]$ and set the parameter-dependent energy norm as

$$\|(v,q)\|_{V\times Q}^2 := \|v\|_V^2 + \|q\|_Q^2 = \|v\|_V^2 + \|q\|_{Q_b}^2 + t^2|q|_c^2.$$

Assume also that the following inf-sup condition holds

$$\|u\|_V \lesssim \sup_{(v,q)\in V\times Q}\frac{a(u,v)+b(v,q)}{\|(v,q)\|_{V\times Q}} \qquad \forall u\in V. \tag{3.2}$$

Then, for every $F\in V'$ and $G\in Q'$, there exists a unique $(u,p)\in V\times Q$ satisfying

$$\begin{aligned} a(u,v)+b(v,p) &= F(v) \qquad \forall v\in V,\\ b(u,q)-t^2c(p,q) &= G(q) \qquad \forall q\in Q. \end{aligned}$$

Furthermore, the following continuous dependence on data holds

$$\|(u,p)\|_{V\times Q} \lesssim \|F\|_{V'} + \|G\|_{Q'}. \tag{3.4}$$

REMARK 3.1. *The form $c(\cdot,\cdot)$ does not require to be bounded in the norm $\|\cdot\|_{Q_b}$. The space Q_b allows us to absorb the dependency of the model parameters directly in the norms, yielding a robust continuous dependence on data. That is, the hidden constant C associated with (3.4) only depends on the constants associated with the Brezzi–Braess conditions (3.1)-(3.2), and the continuity constants.*

3.1. Unique solvability of the decoupled sub-problems. In this section, we verify that the assumptions of Theorem 3.1 are satisfied for (2.10) and (2.11). While some of the arguments employed in these proofs are standard, we prefer to write them down explicitly for the sake of completeness.

Let us adopt the following notation for the functional spaces for displacement and total volumetric stress $\mathbf{V}_1 := \mathbf{H}^1_D(\Omega)$ and $Q_1 = Q_{b_1} := L^2(\Omega)$, equipped with the following scaled norms and seminorms

$$\|\boldsymbol{u}\|_{\mathbf{V}_1}^2 := 2\mu\|\boldsymbol{\varepsilon}(\boldsymbol{u})\|_{0,\Omega}^2, \quad \|\tilde{p}\|_{Q_1}^2 := \|\tilde{p}\|_{Q_{b_1}}^2 + \frac{1}{\lambda}|\tilde{p}|_{c_1}^2, \quad \|\tilde{p}\|_{Q_{b_1}}^2 := \frac{1}{2\mu}\|\tilde{p}\|_{0,\Omega}^2, \quad |\tilde{p}|_{c_1}^2 := \|\tilde{p}\|_{0,\Omega}^2.$$

On the other hand, let us denote the functional spaces for diffusive flux and concentration as $\mathbf{V}_2 = \mathbf{H}_N(\mathrm{div},\Omega)$ and $Q_2 = Q_{b_2} = L^2(\Omega)$, furnished with the following norms and seminorms

$$\begin{aligned} &\|\boldsymbol{\zeta}\|_{\mathbf{V}_2}^2 := \|\boldsymbol{\zeta}\|_{\mathbb{M}}^2 + M\|\mathrm{div}\,\boldsymbol{\zeta}\|_{0,\Omega}^2, \quad \|\varphi\|_{Q_2}^2 := \|\varphi\|_{Q_{b_2}}^2 + \theta|\varphi|_{c_2}^2,\\ &\|\boldsymbol{\zeta}\|_{\mathbb{M}}^2 := a_2^{\boldsymbol{w},\tilde{r}}(\boldsymbol{\zeta},\boldsymbol{\zeta}), \quad \|\varphi\|_{Q_{b_2}}^2 := \frac{1}{M}\|\varphi\|_{0,\Omega}^2, \quad |\varphi|_{c_2}^2 := \|\varphi\|_{0,\Omega}^2. \end{aligned}$$

LEMMA 3.2. *For a fixed $\vartheta\in Q_2$, assume that $1\le\lambda$ and $0<\mu$. Then, there exists a unique solution $(\boldsymbol{u},\tilde{p})\in\mathbf{V}_1\times Q_1$ to (2.10).*

Proof. Clearly, Q_1 is a dense linear subspace of Q_{b_1} with the respective norms. Thanks to Körn's inequality we readily have that $\|\boldsymbol{\varepsilon}(\boldsymbol{v})\|_{0,\Omega}$ forms an equivalent norm to the standard $\mathbf{H}^1_D$-norm in $\mathbf{V}_1$. Next, we invoke the Cauchy–Schwarz inequality to conclude the continuity of $a_1(\cdot,\cdot)$ on $\mathbf{V}_1$:

$$|a_1(\boldsymbol{u},\boldsymbol{v})| = \left|2\mu\int_\Omega \boldsymbol{\varepsilon}(\boldsymbol{u}):\boldsymbol{\varepsilon}(\boldsymbol{v})\right| \le 2\mu\|\boldsymbol{\varepsilon}(\boldsymbol{u})\|_{0,\Omega}\|\boldsymbol{\varepsilon}(\boldsymbol{v})\|_{0,\Omega} = \|\boldsymbol{u}\|_{\mathbf{V}_1}\|\boldsymbol{v}\|_{\mathbf{V}_1} \quad \forall \boldsymbol{u},\boldsymbol{v}\in\mathbf{V}_1.$$

In addition, by definition of $\|\cdot\|_{\mathbf{V}_1}$, we have that $a_1(\cdot,\cdot)$ is symmetric, positive semi-definite and coercive in $\mathbf{V}_1$ (giving, in particular, condition (3.1a)). The Cauchy–Schwarz inequality, the triangle inequality $\|\operatorname{div}\boldsymbol{v}\|_{0,\Omega} \le \|\nabla\boldsymbol{v}\|_{0,\Omega}$, and Körn's inequality implies the continuity of $b_1(\cdot,\cdot)$ on $\mathbf{V}_1 \times Q_{b_1}$ as follows

$$|b_1(\boldsymbol{v},\tilde{q})| = \left| -\int_\Omega \tilde{q}\operatorname{div}\boldsymbol{v}\right| \le \|\tilde{q}\|_{0,\Omega}\|\operatorname{div}\boldsymbol{v}\|_{0,\Omega} \lesssim \|\tilde{q}\|_{0,\Omega}\|\boldsymbol{\varepsilon}(\boldsymbol{v})\|_{0,\Omega} = \|\tilde{q}\|_{Q_{b_1}}\|\boldsymbol{v}\|_{\mathbf{V}_1} \quad \forall \tilde{q}\in Q_{b_1}, \forall \boldsymbol{v}\in\mathbf{V}_1.$$

Thanks to the structure of the problem and of the scaled norms, in the context of Theorem 3.1 we can identify $t = \frac{1}{\sqrt{\lambda}} \in (0,1]$, since $1 \le \lambda$. Moreover, $c_1(\cdot,\cdot) = (\cdot,\cdot)_{L^2(\Omega)}$ is symmetric and positive semi-definite. On the other hand, Körn's and Cauchy–Schwarz inequalities imply that

$$|F_1(\boldsymbol{v})| = \left|\int_\Omega \boldsymbol{f}\cdot\boldsymbol{v}\right| \le \|\boldsymbol{f}\|_{0,\Omega}\|\boldsymbol{v}\|_{0,\Omega} \lesssim \|\boldsymbol{f}\|_{0,\Omega}\|\boldsymbol{\varepsilon}(\boldsymbol{v})\|_{0,\Omega} = \|\boldsymbol{f}\|_{Q_{b_1}}\|\boldsymbol{v}\|_{\mathbf{V}_1} \quad \forall \boldsymbol{v}\in\mathbf{V}_1.$$

Similarly, for a given $\vartheta \in Q_2$, the property (2.8) and Cauchy–Schwarz inequality leads to

$$\left|G_1^\vartheta(\tilde{q})\right| = \left|-\frac{1}{\lambda}\int_\Omega \ell(\vartheta)\tilde{q}\right| \le \frac{1}{\lambda}\|\ell(\vartheta)\|_{0,\Omega}\|\tilde{q}\|_{0,\Omega} \lesssim \|\vartheta\|_{Q_1}\|\tilde{q}\|_{Q_1} \quad \forall \tilde{q}\in Q_1,$$

and this yields that $G_1^\vartheta(\cdot)$ is continuous in Q_1. For condition (3.1b), note that the surjectivity of the divergence operator $\operatorname{div} : \mathbf{H}^1_D(\Omega) \to L^2(\Omega)$ (see [13, Lemma 53.9]) gives the following inf-sup condition

$$\|\tilde{q}\|_{0,\Omega} \lesssim \sup_{\boldsymbol{v}\in\mathbf{H}^1_D(\Omega)} \frac{b_1(\boldsymbol{v},\tilde{q})}{\|\nabla\boldsymbol{v}\|_{0,\Omega}} \qquad \forall \tilde{q}\in L^2(\Omega).$$

Scaling this bound with $\frac{1}{\sqrt{2\mu}}$, and using the equivalence between $\|\boldsymbol{\varepsilon}(\boldsymbol{v})\|_{0,\Omega}$ and $\|\nabla\boldsymbol{v}\|_{0,\Omega}$ we obtain

$$\|\tilde{q}\|_{Q_{b_1}} \lesssim \sup_{\boldsymbol{v}\in\mathbf{V}_1} \frac{b_1(\boldsymbol{v},\tilde{q})}{\|\boldsymbol{v}\|_{\mathbf{V}_1}} \qquad \forall \tilde{q}\in Q_{b_1}.$$

Finally, the inf-sup condition (3.2) is obtained as follows, for $\boldsymbol{u}\in\mathbf{V}_1$, let $\boldsymbol{v} = \boldsymbol{u}$ and $\tilde{q} = 0$. We have

$$a_1(\boldsymbol{u},\boldsymbol{u}) + b_1(\boldsymbol{u},0) = a_1(\boldsymbol{u},\boldsymbol{u}) = \|\boldsymbol{u}\|^2_{\mathbf{V}_1} \quad \text{and} \quad \|(\boldsymbol{u},0)\|^2_{\mathbf{V}_1\times Q_1} = \|\boldsymbol{u}\|^2_{\mathbf{V}_1}.$$

Therefore,

$$\|\boldsymbol{u}\|_{\mathbf{V}_1} \lesssim \sup_{(\boldsymbol{v},\tilde{q})\in\mathbf{V}_1\times Q_1} \frac{a_1(\boldsymbol{u},\boldsymbol{v}) + b_1(\boldsymbol{v},\tilde{q})}{\|(\boldsymbol{v},\tilde{q})\|_{\mathbf{V}_1\times Q_1}} \qquad \forall \boldsymbol{u}\in\mathbf{V}_1,$$

verifying the conditions of Theorem 3.1. Then the unique solution satisfies

$$\|(\boldsymbol{u},\tilde{p})\|_{\mathbf{V}_1\times Q_1} \le C_1\left(\|F_1\|_{\mathbf{V}_1'} + \|G_1^\vartheta\|_{Q_1'}\right), \tag{3.5}$$

where the constant $C_1 > 0$ does not depend on the physical parameters. ∎

Lemma 3.3. *For a fixed pair $(\boldsymbol{w},\tilde{r}) \in \mathbf{V}_1\times Q_1$, assume that $0 \le \theta < \frac{1}{M} \le 1$. Then, there exists a unique pair $(\boldsymbol{\xi},\varphi)\in\mathbf{V}_2\times Q_2$ solution to (2.11).*

Proof. It is straightforward to see that Q_{b_2} is a dense linear subspace of Q_2 with the corresponding norms. From the properties of $\mathbb{M}$ in (2.7), for given $(\boldsymbol{w},\tilde{r})\in\mathbf{V}_1\times Q_1$, the norm $\|\cdot\|_{\mathbf{V}_2}$ is a equivalent norm in $\mathbf{H}_N(\operatorname{div},\Omega)$ since $\frac{1}{M}\|\cdot\|^2_{0,\Omega} \le \|\cdot\|^2_{\mathbb{M}} \le M\|\cdot\|^2_{0,\Omega}$. Therefore, the bilinear form $a_2^{\boldsymbol{w},\tilde{r}}(\cdot,\cdot)$ is positive semi-definite, continuous over $\mathbf{V}_2$, and coercive in the nullspace of the linear operator B_2

$$\operatorname{Ker}(B_2) = \{\boldsymbol{\xi}\in\mathbf{V}_2 : \int_\Omega \varphi\operatorname{div}\boldsymbol{\xi} = 0, \forall\varphi\in Q_2\} = \{\boldsymbol{\xi}\in\mathbf{V}_2 : \operatorname{div}\boldsymbol{\xi} = 0\}.$$

Indeed, from Cauchy–Schwarz inequality and the definition of the $\mathbf{V}_2$-norm, we obtain

$$\left|a_2^{\boldsymbol{w},\tilde{r}}(\boldsymbol{\zeta},\boldsymbol{\xi})\right| = \left|\int_\Omega \mathbb{M}^{-1}(\boldsymbol{\varepsilon}(\boldsymbol{w}),\tilde{r})\boldsymbol{\zeta}\cdot\boldsymbol{\xi}\right| \le \|\boldsymbol{\zeta}\|_{\mathbb{M}}\|\boldsymbol{\xi}\|_{\mathbb{M}} \le \|\boldsymbol{\zeta}\|_{\mathbf{V}_2}\|\boldsymbol{\xi}\|_{\mathbf{V}_2} \quad \forall\boldsymbol{\xi},\boldsymbol{\zeta}\in\mathbf{V}_2,$$

and from the characterisation of the Kernel, condition (3.1a) is fulfilled as follows

$$\left|a_2^{\boldsymbol{w},\tilde{r}}(\hat{\boldsymbol{\zeta}},\hat{\boldsymbol{\zeta}})\right| = \left|\int_\Omega \mathbb{M}^{-1}(\boldsymbol{\varepsilon}(\boldsymbol{w}),\tilde{r})\hat{\boldsymbol{\zeta}}\cdot\hat{\boldsymbol{\zeta}}\right| = \|\hat{\boldsymbol{\zeta}}\|^2_{\mathbf{V}_2} \quad \forall\hat{\boldsymbol{\zeta}}\in\operatorname{Ker}(B_2).$$

In addition, from Cauchy–Schwarz inequality and the definition of the norms we are arrive at

$$|b_2(\boldsymbol{\zeta},\psi)| = \left|-\int_\Omega \psi \operatorname{div}\boldsymbol{\zeta}\right| \le \|\psi\|_{0,\Omega}\|\operatorname{div}\boldsymbol{\zeta}\|_{0,\Omega} \le \|\psi\|_{Q_{b_2}}\|\boldsymbol{\zeta}\|_{\mathbf{V}_2} \quad \forall\psi\in Q_{b_2}, \forall\boldsymbol{\zeta}\in\mathbf{V}_2.$$

Furthermore, the bilinear operator $c_2(\cdot,\cdot)$ coincides with $(\cdot,\cdot)_{L^2(\Omega)}$ which is symmetric and positive semi-definite and $t=\sqrt{\theta}\in[0,1]$. Next, the trace inequality together with the equivalence between $\|\boldsymbol{\xi}\|_{\operatorname{div},\Omega}$ and $\|\boldsymbol{\xi}\|_{\mathbf{V}_2}$ yields the continuity of $F_2(\cdot)$ on $\mathbf{V}_2$ as follows

$$|F_2(\boldsymbol{\xi})| = \left|\langle\varphi_D,\boldsymbol{\xi}\cdot\boldsymbol{n}\rangle_{\Gamma_D}\right| \le \|\varphi_D\|_{\frac12,\Gamma_D}\|\boldsymbol{\xi}\|_{\operatorname{div},\Omega} \le \sqrt{M}\|\varphi_D\|_{\frac12,\Gamma_D}\|\boldsymbol{\xi}\|_{\mathbf{V}_2} \quad \forall\boldsymbol{\xi}\in\mathbf{V}_2.$$

Likewise, $G_2(\cdot)$ is continuous on Q_2. Indeed,

$$|G_2(\psi)| = \left|-\int_\Omega g\psi\right| \le \|g\|_{0,\Omega}\|\psi\|_{0,\Omega} = \sqrt{M}\|g\|_{0,\Omega}\|\psi\|_{Q_2} \quad \forall\psi\in Q_2.$$

To prove condition (3.1b), note that the divergence operator $\operatorname{div}:\mathbf{H}_N(\operatorname{div},\Omega)\to L^2(\Omega)$ is surjective (see [13, Lemma 53.9]). Consequently, we obtain an inf-sup condition in non-weighted norms, which is then multiplied by $\frac{1}{\sqrt{M}}$, giving

$$\|\varphi\|_{Q_{b_2}} \lesssim \sup_{\boldsymbol{\zeta}\in\mathbf{V}_2}\frac{b_2(\boldsymbol{\zeta},\varphi)}{\|\boldsymbol{\zeta}\|_{\mathbf{V}_2}} \qquad \forall\varphi\in Q_{b_2}.$$

Lastly, we verify the Braess condition (3.2) as follows: for $\boldsymbol{\zeta}\in\mathbf{V}_2$, let $\boldsymbol{\xi}=\boldsymbol{\zeta}$ and $\varphi=M\operatorname{div}\boldsymbol{\zeta}$, then

$$a_2^{\boldsymbol{w},\tilde r}(\boldsymbol{\zeta},\boldsymbol{\zeta}) + b_2(\boldsymbol{\zeta},M\operatorname{div}\boldsymbol{\zeta}) = a_2^{\boldsymbol{w},\tilde r}(\boldsymbol{\zeta},\boldsymbol{\zeta}) + Mb_2(\boldsymbol{\zeta},\operatorname{div}\boldsymbol{\zeta}) = \|\boldsymbol{\zeta}\|_{\mathbf{V}_2}^2,$$
$$\|(\boldsymbol{\zeta},M\operatorname{div}\boldsymbol{\zeta})\|^2_{\mathbf{V}_2\times Q_2} = \|\boldsymbol{\zeta}\|^2_{\mathbf{V}_2} + \|M\operatorname{div}\zeta\|^2_{Q_{b_2}} + \theta|M\operatorname{div}\boldsymbol{\zeta}|^2_{c_2} \lesssim \|\boldsymbol{\zeta}\|^2_{\mathbf{V}_2} + \frac{1}{M}\|M\operatorname{div}\boldsymbol{\zeta}\|^2_{0,\Omega} \lesssim \|\boldsymbol{\zeta}\|^2_{\mathbf{V}_2}.$$

Therefore,

$$\|\boldsymbol{\zeta}\|_{\mathbf{V}_2} \lesssim \sup_{(\boldsymbol{\xi},\varphi)\in\mathbf{V}_2\times Q_2}\frac{a_2^{\boldsymbol{w},\tilde r}(\boldsymbol{\zeta},\boldsymbol{\xi}) + b_2(\boldsymbol{\xi},\varphi)}{\|(\boldsymbol{\xi},\varphi)\|_{\mathbf{V}_2\times Q_2}} \qquad \forall\boldsymbol{\zeta}\in\mathbf{V}_2.$$

This verifies the conditions in Theorem 3.1 and therefore we also have

$$\|(\boldsymbol{\zeta},\varphi)\|_{\mathbf{V}_2\times Q_2} \le C_2\left(\|F_2\|_{\mathbf{V}_2'} + \|G_2\|_{Q_2'}\right), \tag{3.6}$$

where the constant $C_2>0$ does not depend on the physical parameters. ◻

REMARK 3.2. *The proofs of Lemmas 3.2 and 3.3 provide further details on parameter requirements. The conditions $0<\mu$ and $1\le\lambda$ are needed to properly define weighted norms and the condition over t^2 in Theorem 3.1 is carried over to $\frac{1}{\lambda}$. On the other hand, the bound $0\le\theta<M^{-1}\le 1$ is fundamental in the proof of (3.2). The weighted norms are well defined, and θ plays the role of t^2 in Theorem 3.1. We could relax the dependence of θ on M, but this would require a much more involved metric for φ [7].*

3.2. Fixed-point strategy. Let us now define the following solution operators

$$\mathcal{S}_1: Q_2\to\mathbf{V}_1\times Q_1, \quad \vartheta\mapsto\mathcal{S}_1(\vartheta) = (\mathcal{S}_{11}(\vartheta),\mathcal{S}_{12}(\vartheta)) := (\boldsymbol{u},\tilde p),$$

where $(\boldsymbol{u},\tilde p)$ is the unique solution to (2.10), confirmed in Section 3.1; and

$$\mathcal{S}_2:\mathbf{V}_1\times Q_1\to\mathbf{V}_2\times Q_2, \quad (\boldsymbol{w},\tilde r)\mapsto\mathcal{S}_2(\boldsymbol{w},\tilde r) = (\mathcal{S}_{21}(\boldsymbol{w},\tilde r),\mathcal{S}_{22}(\boldsymbol{w},\tilde r)) := (\boldsymbol{\zeta},\varphi),$$

where $(\boldsymbol{\zeta},\varphi)$ is the unique solution to (2.11), also confirmed in Section 3.1.

The nonlinear problem (2.6) is thus equivalent to the following fixed-point equation:

$$\text{Find } \varphi\in Q_2 \text{ such that } \mathcal{A}(\varphi)=\varphi,$$

where $\mathcal{A}: Q_2\to Q_2$ is defined as $\varphi\mapsto\mathcal{A}(\varphi) := (\mathcal{S}_{22}\circ\mathcal{S}_1)(\varphi)$. Next, we show the Lipschitz continuity of $\mathcal{A}$, i.e., the Lipschitz continuity of the solution operators $\mathcal{S}_1$ and $\mathcal{S}_2$.

LEMMA 3.4. *The operator $\mathcal{S}_1$ is Lipschitz continuous with Lipschitz constant $L_{\mathcal{S}_1}=\sqrt{M}C_1L_\ell$.*

Proof. Let $\vartheta_1, \vartheta_2 \in Q_2$ and $(\boldsymbol{u}_1, \tilde{p}_1), (\boldsymbol{u}_2, \tilde{p}_2)$ be the unique solutions to the problem (2.10). Define the following auxiliary problem: find $(\boldsymbol{u}, \tilde{p}) \in \mathbf{V}_1 \times Q_1$ such that

$$\begin{aligned} a_1(\boldsymbol{u}, \boldsymbol{v}) + b_1(\boldsymbol{v}, \tilde{p}) &= 0 \qquad \forall \boldsymbol{v} \in \mathbf{V}_1, \\ b_1(\boldsymbol{u}, \tilde{q}) - \frac{1}{\lambda} c_1(\tilde{p}, \tilde{q}) &= (G_1^{\vartheta_1} - G_1^{\vartheta_2})(\tilde{q}) \qquad \forall \tilde{q} \in Q_1. \end{aligned}$$

Note that $G_1^{\vartheta_1} - G_1^{\vartheta_2} \in Q_1'$. Then, the unique solution is given by $(\boldsymbol{u}, \tilde{p}) = (\boldsymbol{u}_1 - \boldsymbol{u}_2, \tilde{p}_1 - \tilde{p}_2)$. Therefore, we apply the continuous dependence on data (3.5) together with (2.9b) to obtain

$$\begin{aligned} \|\mathcal{S}_1(\vartheta_1) - \mathcal{S}_1(\vartheta_2)\|_{\mathbf{V}_1 \times Q_1} &= \|(\boldsymbol{u}_1 - \boldsymbol{u}_2, \tilde{p}_1 - \tilde{p}_2)\|_{\mathbf{V}_1 \times Q_1} \\ &\leq C_1 \sup_{\tilde{q} \in Q_1} \frac{|(G_1^{\vartheta_1} - G_1^{\vartheta_2})(\tilde{q})|}{\|\tilde{q}\|_{Q_1}} \leq C_1 \|\ell(\vartheta_1) - \ell(\vartheta_2)\|_{0,\Omega} \\ &\leq C_1 L_\ell \|\vartheta_1 - \vartheta_2\|_{0,\Omega} \leq \sqrt{M} C_1 L_\ell \|\vartheta_1 - \vartheta_2\|_{Q_2}, \end{aligned}$$

where the norm equivalence has been used in the last step. □

LEMMA 3.5. *The operator $\mathcal{S}_2$ is Lipschitz continuous with Lipschitz constant*

$$L_{\mathcal{S}_2} = \max\left\{\frac{1}{\sqrt{2\mu}}, \sqrt{2\mu}\right\} \sqrt{M^3} C_2^2 L_{\mathbb{M}} \left(\|\varphi_D\|_{\frac{1}{2},\Gamma_D} + \|g\|_{0,\Omega}\right).$$

Proof. Analogously, as in Lemma 3.4, let $(\boldsymbol{w}_1, \tilde{r}_1), (\boldsymbol{w}_2, \tilde{r}_2) \in \mathbf{V}_1 \times Q_1$ be such that $(\boldsymbol{\zeta}_1, \varphi_1), (\boldsymbol{\zeta}_2, \varphi_2)$ are the unique solutions of their respective problem (2.11) and consider the following auxiliary problem: find $(\boldsymbol{\zeta}, \varphi) \in \mathbf{V}_2 \times Q_2$ such that

$$\begin{aligned} a_2^{\boldsymbol{w}_1, \tilde{r}_1}(\boldsymbol{\zeta}, \boldsymbol{\xi}) + b_2(\boldsymbol{\xi}, \varphi) &= F^*(\boldsymbol{\xi}) \qquad \forall \boldsymbol{\xi} \in \mathbf{V}_2, \\ b_2(\boldsymbol{\zeta}, \psi) - \theta c_2(\varphi, \psi) &= 0 \qquad \forall \psi \in Q_2, \end{aligned}$$

where $F^*(\boldsymbol{\xi}) = \int_\Omega (\mathbb{M}^{-1}(\boldsymbol{\varepsilon}(\boldsymbol{w}_1), \tilde{r}_1) - \mathbb{M}^{-1}(\boldsymbol{\varepsilon}(\boldsymbol{w}_2), \tilde{r}_2)) \boldsymbol{\zeta}_2 \cdot \boldsymbol{\xi}$. The problem above results from subtracting the problems associated with $(\boldsymbol{w}_1, \tilde{r}_1)$ and $(\boldsymbol{w}_2, \tilde{r}_2)$ and rewriting $a_2^{\boldsymbol{w}_1, \tilde{r}_1}(\boldsymbol{\zeta}_2, \boldsymbol{\xi})$ in the first equation. Note that $F^*(\boldsymbol{\xi}) \in \mathbf{V}_2'$. Therefore, thanks to Lemma 3.3, the unique solution is given by $(\boldsymbol{\zeta}, \varphi) = (\boldsymbol{\zeta}_1 - \boldsymbol{\zeta}_2, \varphi_1 - \varphi_2)$. Using (3.6), Hölder's inequality and (2.9a) we get

$$\begin{aligned} &\|\mathcal{S}_2(\boldsymbol{w}_1, \tilde{r}_1) - \mathcal{S}_2(\boldsymbol{w}_2, \tilde{r}_2)\|_{\mathbf{V}_2 \times Q_2} = \|(\boldsymbol{\zeta}_1 - \boldsymbol{\zeta}_2, \varphi_1 - \varphi_2)\|_{\mathbf{V}_2 \times Q_2} \leq C_2 \sup_{\boldsymbol{\xi} \in \mathbf{V}_2} \frac{|F^*(\boldsymbol{\xi})|}{\|\boldsymbol{\xi}\|_{\mathbf{V}_2}} \\ &\leq \sqrt{M} C_2 \|\mathbb{M}^{-1}(\boldsymbol{\varepsilon}(\boldsymbol{w}_1), \tilde{r}_1) - \mathbb{M}^{-1}(\boldsymbol{\varepsilon}(\boldsymbol{w}_2), \tilde{r}_2)\|_{\infty,\Omega} \|\boldsymbol{\zeta}_2\|_{0,\Omega} \\ &\leq M C_2 L_{\mathbb{M}} \|(\boldsymbol{\varepsilon}(\boldsymbol{w}_1), \tilde{r}_1) - (\boldsymbol{\varepsilon}(\boldsymbol{w}_2), \tilde{r}_2)\|_{\mathbb{L}^2(\Omega) \times L^2(\Omega)} (\|\boldsymbol{\zeta}_2\|_{\mathbf{V}_2} + \|\varphi_2\|_{Q_2}) \\ &\leq \max\left\{\frac{1}{\sqrt{2\mu}}, \sqrt{2\mu}\right\} \sqrt{M^3} C_2^2 L_{\mathbb{M}} \left(\|\varphi_D\|_{\frac{1}{2},\Gamma_D} + \|g\|_{0,\Omega}\right) \|(\boldsymbol{w}_1, \tilde{r}_1) - (\boldsymbol{w}_2, \tilde{r}_2)\|_{\mathbf{V}_1 \times Q_1}. \end{aligned}$$

□

LEMMA 3.6. *The operator $\mathcal{A}$ is Lipschitz continuous with Lipschitz constant $L_{\mathcal{A}} = L_{\mathcal{S}_2} L_{\mathcal{S}_1}$.*

Proof. We can combine the results from Lemmas 3.4 and 3.5 to assert that

$$\begin{aligned} \|\mathcal{A}(\varphi_1) - \mathcal{A}(\varphi_2)\|_{Q_2} &= \|\mathcal{S}_{22}(\mathcal{S}_1(\varphi_1)) - \mathcal{S}_{22}(\mathcal{S}_1(\varphi_2))\|_{Q_2} \\ &\leq L_{\mathcal{S}_2} \|\mathcal{S}_1(\varphi_1) - \mathcal{S}_1(\varphi_2)\|_{\mathbf{V}_1 \times Q_1} \leq L_{\mathcal{S}_2} L_{\mathcal{S}_1} \|\varphi_1 - \varphi_2\|_{Q_2}, \end{aligned}$$

for any $\varphi_1, \varphi_2 \in Q_2$, where we have also used the definition of the solution operators. □

Finally, let us define the following set

$$\mathbf{W} = \left\{\boldsymbol{w} \in Q_2 \colon \|w\|_{Q_2} \leq \sqrt{M} C_2 \left(\|\varphi_D\|_{\frac{1}{2},\Gamma_D} + \|g\|_{0,\Omega}\right)\right\}, \tag{3.7}$$

and note that the operator $\mathcal{A}$ satisfies that $\mathcal{A}(\mathbf{W}) \subseteq \mathbf{W}$. Indeed, from the continuous dependence on data (3.6), it is readily seen that

$$\|A(\varphi)\|_{Q_2} = \|S_{22}(S_1(\varphi))\|_{Q_2} \leq \|S_2(S_1(\varphi))\|_{\mathbf{V}_2 \times Q_2} \leq \sqrt{M} C_2 \left(\|\varphi_D\|_{\frac{1}{2},\Gamma_D} + \|g\|_{0,\Omega}\right).$$

The following theorem provides the well-posedness of the coupled problem.

THEOREM 3.7. *Let $\mathbf{W}$ be as in (3.7) and assume that $L_{\mathcal{A}} < 1$. Then the operator $\mathcal{A}$ has a unique fixed point $\varphi \in \mathbf{W}$. Equivalently, the coupled problem (2.6) has an unique solution $(\boldsymbol{u}, \tilde{p}, \boldsymbol{\zeta}, \varphi) \in \mathbf{V}_1 \times Q_1 \times \mathbf{V}_2 \times Q_2$ and the following continuous dependence on data holds*

$$\|(\boldsymbol{u}, \tilde{p})\|_{\mathbf{V}_1 \times Q_1} \leq C_1 \left(\|F_1\|_{\mathbf{V}_1'} + \|G_1^{\varphi}\|_{Q_1'}\right), \tag{3.8a}$$

$$\|(\boldsymbol{\zeta}, \varphi)\|_{\mathbf{V}_2 \times Q_2} \leq C_2 \left(\|F_2\|_{\mathbf{V}_2'} + \|G_2\|_{Q_2'}\right), \tag{3.8b}$$

where the corresponding constants C_1 and C_2 do not depend on the physical parameters.

Proof. It follows directly from Lemma 3.6 together with the Banach fixed-point theorem. □

4. Virtual element discretisation. The aim of this section is to introduce and analyse a VEM for each decoupled problem (2.10) and (2.11) based on [2, 3, 4]. Next, similarly as for the continuous problem, we employ a discrete fixed-point argument to prove the well-posedness of the coupled discrete problem.

Mesh assumptions and recurrent notation. Let $\mathcal{T}_h$ be a decomposition of Ω into polygonal elements E with diameter h_E and let $\mathcal{E}_h$ be the set of edges e of $\mathcal{T}_h$ with length h_e. We assume that for every E there exists $\rho_E > 0$ such that E is star-shaped with respect to every point of a disk with radius $\rho_E h_E$ and in addition $h_e \geq \rho_E h_E$ for every edge e of E. When considering a sequence $\{\mathcal{T}_h\}_h$ we assume that $\rho_E \geq \rho > 0$ for some ρ independent of E, where h is the maximum diameter over $\mathcal{T}_h$.

Given an integer $k \geq 0$ the space of polynomials of grade $\leq k$ on E is denoted by $\mathcal{P}_k(E)$ and the space of the gradients of polynomials of grade $\leq k+1$ on E is denoted as $\mathcal{G}_k(E) := \nabla \mathcal{P}_{k+1}(E)$ with standard notation $\mathcal{P}_{-1}(E) = \{0\}$ for $k = -1$. The space $\mathcal{G}_k^{\oplus}(E)$ denotes the complement of the space $\mathcal{G}_k(E)$ in the vector polynomial space $(\mathcal{P}_k(E))^2$, that is, $(\mathcal{P}_k(E))^2 = \mathcal{G}_k(E) \oplus \mathcal{G}_k^{\oplus}(E)$. Next we define the continuous space of polynomials along the boundary ∂E of E as

$$\mathcal{B}_k(\partial E) := \left\{v \in C^0(\partial E) \colon v|_e \in \mathcal{P}_k(e), \quad \forall e \subset \partial E\right\}.$$

Let $\boldsymbol{x}_E = (x_E, y_E)$ denote the barycentre of E and let $\mathcal{M}_k(E)$ be the set of $(k+1)(k+2)/2$ scaled monomials

$$\mathcal{M}_k(E) := \left\{\left(\frac{\boldsymbol{x} - \boldsymbol{x}_E}{h_E}\right)^{\mathbf{t}}, 0 \leq |\mathbf{t}| \leq k\right\},$$

where $\mathbf{t} = (t_1, t_2)$ is a non-negative multi-index with $|\mathbf{t}| = t_1 + t_2$ and $\boldsymbol{x}^{\mathbf{t}} = x^{t_1} y^{t_2}$ for $\boldsymbol{x} = (x, y)$. In particular, we can take the basis of $\mathcal{G}_k(E)$ and $\mathcal{G}_k^{\oplus}(E)$ as $\mathcal{M}_k^{\nabla}(E) := \nabla \mathcal{M}_{k+1}(E) \setminus \{\mathbf{0}\}$ and $\mathcal{M}_k^{\oplus}(E) := (\nabla \mathcal{M}_{k+1}(E) \setminus \{\mathbf{0}\})^{\oplus}$, respectively, with $(\mathcal{M}_k(E))^2 = \mathcal{M}_k^{\nabla}(E) \oplus \mathcal{M}_k^{\oplus}(E)$.

4.1. Discrete formulation for the elasticity problem. In order to state the discrete spaces for (2.10) we adapt the approach from [4] to our formulation which involves the presence of the operator $\boldsymbol{\varepsilon}$ in the bilinear form $a_1(\cdot,\cdot)$ and the active-stress term $\ell(\vartheta)$ in $G_1^{\vartheta}(\cdot)$.

Discrete spaces and degrees of freedom. For $k_1 \geq 2$, the VE space for displacement locally solves the Stokes problem and is defined by

$$\begin{aligned}\mathbf{V}_1^{h,k_1}(E) = \{\boldsymbol{v} \in \mathbf{H}^1(E) \colon \boldsymbol{v}|_{\partial E} \in (\mathcal{B}_{k_1}(\partial E))^2,\ \operatorname{div} \boldsymbol{v} \in \mathcal{P}_{k_1-1}(E),\\ - 2\mu\, \mathbf{div}\, \boldsymbol{\varepsilon}(\boldsymbol{v}) - \nabla s \in \mathcal{G}_{k_1-2}^{\oplus}(E) \text{ for some } s \in L_0^2(E)\}.\end{aligned}$$

Observe that $(\mathcal{P}_{k_1}(E))^2 \subseteq \mathbf{V}_1^{h,k_1}(E)$. For the discrete pressure space $Q_1^{h,k_1}(E)$, we can just locally consider the polynomials $\mathcal{P}_{k_1-1}(E)$. Then, the global discrete spaces are defined as

$$\mathbf{V}_1^{h,k_1} = \{\boldsymbol{v} \in \mathbf{V}_1 \colon \boldsymbol{v}|_E \in \mathbf{V}_1^{h,k_1}(E),\ \forall E \in \mathcal{T}_h\}, \qquad Q_1^{h,k_1} = \{\tilde{q} \in Q_1 \colon \tilde{q}|_E \in Q_1^{h,k_1}(E),\ \forall E \in \mathcal{T}_h\}.$$

The DoFs for $\boldsymbol{v}_h \in \mathbf{V}_1^{h,k_1}(E)$ can be taken as follows

- The values of $\boldsymbol{v}_h$ at the vertices of E, (4.1a)
- The values of $\boldsymbol{v}_h$ on the $k_1 - 1$ internal Gauss–Lobatto quadrature points on each edge of E, (4.1b)
- $\displaystyle\int_E (\operatorname{div} \boldsymbol{v}_h) m_{k_1-1}, \quad \forall m_{k_1-1} \in \mathcal{M}_{k_1-1}(E) \setminus \{1\},$ (4.1c)
- $\displaystyle\int_E \boldsymbol{v}_h \cdot \mathbf{m}_{k_1-2}^{\oplus}, \quad \forall \mathbf{m}_{k_1-2}^{\oplus} \in \mathcal{M}_{k_1-2}^{\oplus}(E).$ (4.1d)

On the other hand, the DoFs for $\tilde{q}_h \in Q_1^{h,k_1}(E)$ are selected as

$$\bullet \int_E \tilde{q}_h m_{k_1-1}, \quad \forall m_{k_1-1} \in \mathcal{M}_{k_1-1}(E). \tag{4.2}$$

The set of DoFs (4.1a)-(4.1d) (resp. (4.2)) are unisolvent for the VE space $\mathbf{V}_1^{h,k_1}(E)$ (resp. $Q_1^{h,k_1}(E)$) (see [4, Proposition 3.1]). Furthermore, if N_e denotes the number of edges of E, it is not difficult to check that

$$\dim(\mathbf{V}_1^{h,k_1}(E)) = 2N_e k_1 + \frac{(k_1-1)(k_1-2)}{2} + \frac{(k_1+1)k_1}{2} - 1, \quad \dim(Q_1^{h,k_1}(E)) = \frac{(k_1+1)k_1}{2}.$$

Projection operators. For $E \in \mathcal{T}_h$, denote the energy projection operator by $\mathbf{\Pi}_1^{\boldsymbol{\varepsilon},k_1} : \mathbf{H}^1(E) \to (\mathcal{P}_{k_1}(E))^2$, defined locally through

$$\int_E \boldsymbol{\varepsilon}(\boldsymbol{v}_h - \mathbf{\Pi}_1^{\boldsymbol{\varepsilon},k_1}\boldsymbol{v}_h) : \boldsymbol{\varepsilon}(\mathbf{m}_{k_1}) = 0 \quad \forall \mathbf{m}_{k_1} \in (\mathcal{M}_{k_1}(E))^2.$$

Note that the above definition of projection involving symmetric gradient leads to $\mathbf{0}$ for polynomials $\mathbf{p} \in \{(1,0),(0,1),(-y,x)\}$. Therefore, we need to impose three additional conditions to uniquely define $\mathbf{\Pi}_1^{\boldsymbol{\varepsilon},k_1}$. For example, we can take the following conditions from [36]

$$\sum_{i=1}^{N_v} (\mathbf{\Pi}_1^{\boldsymbol{\varepsilon},k_1}\boldsymbol{v}_h(z_i), \mathbf{p}(z_i)) = \sum_{i=1}^{N_v} (\boldsymbol{v}_h(z_i), \mathbf{p}(z_i)), \quad \forall \mathbf{p} \in \{(1,0),(0,1),(-y,x)\},$$

where N_v is the total number of vertices z_i of E. Moreover, the projection $\mathbf{\Pi}_1^{\boldsymbol{\varepsilon},k_1}\boldsymbol{v}_h$ is computable for $\boldsymbol{v}_h \in \mathbf{V}_1^{h,k_1}(E)$ from (4.1) (see [4, Section 3.2]). We also introduce the L^2-projection $\mathbf{\Pi}_1^{0,k_1} : \mathbf{L}^2(E) \to (\mathcal{P}_{k_1}(E))^2$ defined locally, for a given $v_h \in \mathbf{L}^2(E)$ and $E \in \mathcal{T}_h$, as

$$\int_E (\boldsymbol{v}_h - \mathbf{\Pi}_1^{0,k_1}\boldsymbol{v}_h) \cdot \mathbf{m}_{k_1} = 0, \quad \forall \mathbf{m}_{k_1} \in (\mathcal{M}_{k_1}(E))^2.$$

Notice that $\mathbf{\Pi}_1^{0,k_1-2}\boldsymbol{v}_h$ can be computed for $\boldsymbol{v}_h \in \mathbf{V}_1^{h,k_1}(E)$ from (4.1) (see [4, Section 3.3]). Finally, the discrete right-hand side is defined as $\boldsymbol{f}_h := \mathbf{\Pi}_1^{0,k_1-2}\boldsymbol{f}$ for $\boldsymbol{f} \in \mathbf{L}^2(\Omega)$.

The following two lemmas are classical projection and interpolation estimates, written here in the scaled norms (for sake of robustness with respect to model parameters). Let us first define the semi-norms induced by the spaces $\mathbf{V}_1$ and Q_{b_1} as

$$|\boldsymbol{v}|_{s_1+1,\mathbf{V}_1}^2 = 2\mu|\boldsymbol{v}|_{s_1+1,\Omega}^2 \quad \text{and} \quad |\tilde{q}|_{s_1+1,Q_{b_1}}^2 = \frac{1}{2\mu}|\tilde{q}|_{s_1+1,\Omega}^2 \quad \text{with} \quad 0 \leq s_1 \leq k_1.$$

Lemma 4.1. *For any $\boldsymbol{v} \in (\mathbf{H}^{s_1+1}(\Omega) \cap \mathbf{V}_1, |\cdot|_{s_1+1,\mathbf{V}_1})$ and $\tilde{q} \in (H^{s_1+1}(\Omega) \cap Q_{b_1}, |\cdot|_{s_1+1,Q_{b_1}})$, the polynomial projections $\mathbf{\Pi}_1^{\boldsymbol{\varepsilon},k_1}\boldsymbol{v}$ and $\Pi_1^{0,k_1}\tilde{q}$ satisfy the following estimates*

$$\|\boldsymbol{v} - \mathbf{\Pi}_1^{\boldsymbol{\varepsilon},k_1}\boldsymbol{v}\|_{\mathbf{V}_1} \lesssim h^{s_1}|\boldsymbol{v}|_{s_1+1,\mathbf{V}_1}, \tag{4.3a}$$

$$\|\tilde{q} - \Pi_1^{0,k_1}\tilde{q}\|_{Q_{b_1}} \lesssim h^{s_1+1}|\tilde{q}|_{s_1+1,Q_{b_1}}. \tag{4.3b}$$

Proof. Note that locally the following estimates hold (see [9])

$$|\boldsymbol{v} - \mathbf{\Pi}_1^{\boldsymbol{\varepsilon},k_1}\boldsymbol{v}|_{1,E} \lesssim h_E^{s_1}|\boldsymbol{v}|_{s_1+1,E}, \quad \|\tilde{p} - \Pi_1^{0,k_1}\tilde{q}\|_{0,E} \lesssim h_E^{s_1+1}|\tilde{q}|_{s_1+1,E}.$$

Therefore, the equivalence between $|\cdot|_{1,\Omega}$ and $\|\cdot\|_{\mathbf{V}_1}$ already discussed in Lemma 3.2 and the additive property of the norm imply that

$$\|\boldsymbol{v} - \mathbf{\Pi}_1^{\boldsymbol{\varepsilon},k_1}\boldsymbol{v}\|_{\mathbf{V}_1} \lesssim \sum_{E\in\mathcal{T}_h} \sqrt{2\mu}|\boldsymbol{v} - \mathbf{\Pi}_1^{\boldsymbol{\varepsilon},k_1}\boldsymbol{v}|_{1,E} \lesssim \sum_{E\in\mathcal{T}_h} h_E^{s_1}\sqrt{2\mu}|\boldsymbol{v}|_{s_1+1,E} \leq h^{s_1}|\boldsymbol{v}|_{s_1+1,\mathbf{V}_1}.$$

Similarly

$$\|\tilde{q} - \Pi_1^{0,k_1}\tilde{q}\|_{Q_{b_1}} = \sum_{E\in\mathcal{T}_h} \frac{1}{\sqrt{2\mu}}\|\tilde{q} - \Pi_1^{0,k_1}\tilde{q}\|_{0,E} \lesssim \sum_{E\in\mathcal{T}_h} h_E^{s_1+1}\frac{1}{\sqrt{2\mu}}|\tilde{q}|_{s_1+1,E} \leq h^{s_1}|\tilde{q}|_{s_1+1,Q_{b_1}}. \qquad \square$$

Interpolation operator. We define the Fortin operator $\boldsymbol{\Pi}_1^{F,k_1} : \mathbf{H}^{1+\delta}(E) \to \mathbf{V}_1^{h,k_1}(E)$ for $\delta > 0$ through the DoFs (4.1) as

$$\mathrm{dof}_j(\boldsymbol{v} - \boldsymbol{\Pi}_1^{F,k_1}\boldsymbol{v}) = 0, \quad \text{for all } j = 1, \ldots, \dim(\mathbf{V}_1^{h,k_1}(E)) \text{ and for any } \boldsymbol{v} \in \mathbf{H}^{1+\delta}(E).$$

Let Π_1^{0,k_1-1} be the L^2-projection of $L^2(E)$ onto the space $\mathcal{P}_{k_1-1}(E)$. From (4.1c), $\operatorname{div} \boldsymbol{\Pi}_1^{F,k_1}\boldsymbol{v} \in \mathcal{P}_{k_1-1}(E)$ and the following commutative property holds

$$\operatorname{div} \boldsymbol{\Pi}_1^{F,k_1}\boldsymbol{v} = \Pi_1^{0,k_1-1} \operatorname{div} \boldsymbol{v}.$$

Lemma 4.2. *Given $\boldsymbol{v} \in (\mathbf{H}^{s_1+1}(\Omega) \cap \mathbf{V}_1), |\cdot|_{s_1+1,\mathbf{V}_1})$, the Fortin interpolation operator $\boldsymbol{\Pi}_1^{F,k_1}$ satisfies*

$$\|\boldsymbol{v} - \boldsymbol{\Pi}_1^{F,k_1}\boldsymbol{v}\|_{\mathbf{V}_1} \lesssim h^{s_1}|\boldsymbol{v}|_{s_1+1,\mathbf{V}_1}. \tag{4.5}$$

Proof. The proof of the standard interpolation estimate

$$|\boldsymbol{v} - \boldsymbol{\Pi}_1^{F,k_1}\boldsymbol{v}|_{1,E} \lesssim h_E^{s_1}|\boldsymbol{v}|_{s_1+1,E}$$

on each element $E \in \mathcal{T}_h$ is provided in [28, Theorem 2.4]. This with the obvious scaling shows that

$$\|\boldsymbol{v} - \boldsymbol{\Pi}_1^{F,k_1}\boldsymbol{v}\|_{\mathbf{V}_1} \lesssim \sum_{E\in\mathcal{T}_h} \sqrt{2\mu}|\boldsymbol{v} - \boldsymbol{\Pi}_1^{F,k_1}\boldsymbol{v}|_{1,E} \lesssim \sum_{E\in\mathcal{T}_h} h_E^{s_1}\sqrt{2\mu}|\boldsymbol{v}|_{s_1+1,E} \le h^{s_1}|\boldsymbol{v}|_{s_1+1,\mathbf{V}_1}. \qquad \square$$

Discrete forms. For $E \in \mathcal{T}_h$, let $a_1^E(\cdot,\cdot)$ be the restriction of $a_1(\cdot,\cdot)$ to E. Then its discrete counterpart is defined, for all $\boldsymbol{u}_h, \boldsymbol{v}_h \in \mathbf{V}_1^{h,k_1}(E)$, by

$$a_1^{h,E}(\boldsymbol{u}_h, \boldsymbol{v}_h) := a_1^E(\boldsymbol{\Pi}_1^{\boldsymbol{\varepsilon},k_1}\boldsymbol{u}_h, \boldsymbol{\Pi}_1^{\boldsymbol{\varepsilon},k_1}\boldsymbol{v}_h) + S_1^E(\boldsymbol{u}_h - \boldsymbol{\Pi}_1^{\boldsymbol{\varepsilon},k_1}\boldsymbol{u}_h, \boldsymbol{v}_h - \boldsymbol{\Pi}_1^{\boldsymbol{\varepsilon},k_1}\boldsymbol{v}_h),$$

where $S_1^E(\cdot,\cdot)$ is any symmetric and positive definite bilinear form defined on $\mathbf{V}_1^{h,k_1}(E) \times \mathbf{V}_1^{h,k_1}(E)$ that scales like $a_1^E(\cdot,\cdot)$. In particular, there holds

$$a_1^E(\boldsymbol{v}_h, \boldsymbol{v}_h) \lesssim S_1^E(\boldsymbol{v}_h, \boldsymbol{v}_h) \lesssim a_1^E(\boldsymbol{v}_h, \boldsymbol{v}_h), \quad \forall \boldsymbol{v}_h \in \ker(\boldsymbol{\Pi}_1^{\boldsymbol{\varepsilon},k_1}). \tag{4.6}$$

Set the global discrete bilinear form as $a_1^h(\boldsymbol{u}_h, \boldsymbol{v}_h) = \sum_{E\in\mathcal{T}_h} a_1^{h,E}(\boldsymbol{u}_h, \boldsymbol{v}_h)$ for all $\boldsymbol{u}_h, \boldsymbol{v}_h \in \mathbf{V}_1^{h,k_1}$. For the linear functional F_1, the corresponding global discrete form $F_1^h(\cdot)$ is defined as

$$F_1^h(\boldsymbol{v}_h) = \int_\Omega \boldsymbol{f} \cdot \boldsymbol{\Pi}_1^{0,k_1-2}\boldsymbol{v}_h \quad \text{for } \boldsymbol{v}_h \in \mathbf{V}_1^{h,k_1}.$$

Notice that the computability of $\boldsymbol{\Pi}_1^{\boldsymbol{\varepsilon},k_1}$ and $\boldsymbol{\Pi}_1^{0,k_1-2}$ implies that of $a_1^{h,E}(\boldsymbol{u}_h, \boldsymbol{v}_h)$ and $F_1^{h,E}(\boldsymbol{v}_h)$. On the other hand, the definition of $\mathbf{V}_1^{h,k_1}$ and Q_1^{h,k_1} allow us to extend the bilinear forms $b_1(\cdot,\cdot)$, $c_1(\cdot,\cdot)$ and $G_1^{\vartheta_h}(\cdot)$ ($\vartheta_h \in Q_2^{h,k_2}$ to be defined explicitly later in (4.8b)) to computable discrete bilinear forms as follows

$$b_1^h(\boldsymbol{v}_h, \tilde{q}_h) = \sum_{E\in\mathcal{T}_h} \int_E \tilde{q}_h \operatorname{div} \boldsymbol{v}_h = b_1(\boldsymbol{v}_h, \tilde{q}_h), \quad c_1^h(\tilde{p}_h, \tilde{q}_h) = \sum_{E\in\mathcal{T}_h} \int_E \tilde{p}_h\tilde{q}_h = c_1(\tilde{p}_h, \tilde{q}_h) \quad \text{and}$$
$$G_1^{\vartheta_h,h}(\tilde{q}_h) = \sum_{E\in\mathcal{T}_h} \int_E \ell(\vartheta_h)\tilde{q}_h = G_1^{\vartheta_h}(\tilde{q}_h),$$

where a proper order in the quadrature rule is used to handle the term $\ell(\vartheta_h)$ in $G_1^{\vartheta_h}(\tilde{p}_h)$.

Discrete formulation. For a given $\vartheta_h \in Q_2^{h,k_2}$, find $(\boldsymbol{u}_h, \tilde{p}_h) \in \mathbf{V}_1^{h,k_1} \times Q_1^{h,k_1}$ such that

$$a_1^h(\boldsymbol{u}_h, \boldsymbol{v}_h) + b_1(\boldsymbol{v}_h, \tilde{p}_h) = F_2^h(\boldsymbol{v}_h) \qquad \forall \boldsymbol{v}_h \in \mathbf{V}_1^{h,k_1}, \tag{4.7a}$$
$$b_1(\boldsymbol{u}_h, \tilde{q}_h) - \frac{1}{\lambda}c_1(\tilde{p}_h, \tilde{q}_h) = G_1^{\vartheta_h}(\tilde{q}_h) \qquad \forall \tilde{p}_h \in Q_1^{h,k_1}. \tag{4.7b}$$

4.2. Virtual element approximation for the reaction-diffusion problem. In order to state the discrete counterpart of (2.11) using VE spaces, we adapt the approach from [3] to our formulation with the stress-assisted diffusion $\mathbb{M}^{-1}(\boldsymbol{\varepsilon}(\boldsymbol{w}), \tilde{r})$ as part of the bilinear form $a_2^{\boldsymbol{w},\tilde{r}}(\cdot,\cdot)$.

VE spaces and DoFs. For $k_2 \geq 0$, the discrete VE space locally solves a div-rot problem, that is,

$$\mathbf{V}_2^{h,k_2}(E) = \{\boldsymbol{\xi} \in \mathbf{H}(\mathrm{div}, E) \cap \mathbf{H}(\mathrm{rot}, E) \colon \boldsymbol{\xi} \cdot \boldsymbol{n}|_e \in \mathcal{P}_{k_2}(e) \text{ for all } e \in \partial E,$$
$$\mathrm{div}\, \boldsymbol{\xi} \in \mathcal{P}_{k_2}(E),\ \mathrm{rot}\, \boldsymbol{\xi} \in \mathcal{P}_{k_2-1}(E)\}.$$

In turn, the global discrete spaces are defined as follows

$$\mathbf{V}_2^{h,k_2} = \{\boldsymbol{\zeta} \in \mathbf{V}_2 \colon \boldsymbol{\zeta}|_E \in \mathbf{V}_2^{h,k_2}(E), \quad \forall E \in \mathcal{T}_h\}, \tag{4.8a}$$
$$Q_2^{h,k_2} = \{\varphi \in Q_2 \colon \varphi|_E \in \mathcal{P}_{k_2}(E), \quad \forall E \in \mathcal{T}_h\}. \tag{4.8b}$$

The DoFs for $\boldsymbol{\xi}_h \in \mathbf{V}_2^{h,k_2}(E)$ can be taken as

- Values of $\boldsymbol{\xi}_h \cdot \boldsymbol{n}$ on the k_2+1 Gauss–Lobatto quadrature points of each edge of E, (4.9a)
- $\displaystyle\int_E \boldsymbol{\xi}_h \cdot \mathbf{m}_{k_2-1}^{\nabla}, \quad \forall \mathbf{m}_{k_2-1}^{\nabla} \in \mathcal{M}_{k_2-1}^{\nabla}(E),$ (4.9b)
- $\displaystyle\int_E \boldsymbol{\xi}_h \cdot \mathbf{m}_{k_2}^{\oplus}, \quad \forall \mathbf{m}_{k_2}^{\oplus} \in \mathcal{M}_{k_2}^{\oplus}(E),$ (4.9c)

whereas the DoFs for $\psi_h \in Q_2^{h,k_2}(E)$ are

$$\bullet \int_E \psi_h m_{k_2}, \quad \forall m_{k_2} \in \mathcal{M}_{k_2}(E). \tag{4.10}$$

Note that $(\mathcal{P}_{k_2}(E))^2 \subseteq \mathbf{V}_2^{h,k_2}(E)$ and $\mathcal{P}_{k_2}(E) = Q_2^{h,k_2}(E)$. The set of DoFs (4.9a)-(4.9c) (resp. (4.10)) are unisolvent for the local virtual space $\mathbf{V}_2^{h,k_2}(E)$ (resp. $Q_2^{h,k_2}(E)$), see [10, Proposition 3.5] for a proof (although the DoFs are slightly different, the proof follows similarly). Moreover, it is readily seen that

$$\dim(\mathbf{V}_2^{h,k_2}(E)) = N_e(k_2+1) + \frac{k_2(k_2-1)}{2} - 1 + \frac{(k_2+2)(k_2+1)}{2}, \quad \dim(Q_2^{h,k_2}(E)) = \frac{(k_2+1)k_2}{2}.$$

Projection operators. Let us define the local L^2-projection $\boldsymbol{\Pi}_2^{0,k_2} : \mathbf{L}^2(E) \to (\mathcal{P}_{k_2}(E))^2$ by

$$\int_E (\boldsymbol{\xi}_h - \boldsymbol{\Pi}_2^{0,k_2}\boldsymbol{\xi}_h) \cdot \mathbf{m}_{k_2} = 0, \quad \forall \mathbf{m}_{k_2} \in (\mathcal{M}_{k_2}(E))^2, \quad \forall E \in \mathcal{T}_h.$$

Note that the projection $\boldsymbol{\Pi}_2^{0,k_2}\boldsymbol{\xi}_h$ is computable for $\boldsymbol{\xi}_h \in \mathbf{V}_2^{h,k_2}(E)$ (see [3, Section 3.2]).

For sake of the forthcoming analysis, let us define semi-norms induced by the spaces $\mathbf{V}_2$ and Q_{b_2} as

$$|\boldsymbol{\xi}|^2_{s_2+1,\mathbf{V}_2} = M|\boldsymbol{\xi}|^2_{s_2+1,\Omega} \quad \text{and} \quad |\psi|^2_{s_2+1,Q_{b_2}} = \frac{1}{M}|\psi|^2_{s_2+1,\Omega}, \quad \text{with} \quad 0 \leq s_2 \leq k_2.$$

Lemma 4.3. *For any $\boldsymbol{\xi} \in (\mathbf{H}^{s_2+1}(\Omega) \cap \mathbf{V}_2, |\cdot|_{s_2+1,\mathbf{V}_2})$ and $\psi \in (H^{s_2+1}(\Omega) \cap Q_{b_2}, |\cdot|_{s_2+2,Q_{b_2}})$, the polynomial projections $\boldsymbol{\Pi}_2^{0,k_2}\boldsymbol{\xi}$ and $\Pi_1^{0,k_2}\psi$ satisfy the following estimates*

$$\|\boldsymbol{\xi} - \boldsymbol{\Pi}_2^{0,k_2}\boldsymbol{\xi}\|_{\mathbb{M}} \lesssim h^{s_2+1}|\boldsymbol{\xi}|_{s_2+1,\mathbf{V}_2}, \quad \|\psi - \Pi_2^{0,k_2}\psi\|_{Q_{b_2}} \lesssim h^{s_2+1}|\psi|_{s_2+1,Q_{b_2}}.$$

Proof. Classical results (see [9]) lead to the bounds

$$\|\boldsymbol{\xi} - \boldsymbol{\Pi}_2^{0,k_2}\boldsymbol{\xi}\|_{0,E} \lesssim h_E^{s_2+1}|\boldsymbol{\xi}|_{s_2+1,E}, \qquad \|\psi - \Pi_2^{0,k_2}\psi\|_{0,E} \lesssim h_E^{s_2+1}|\psi|_{s_2+1,E}.$$

Since $\|\cdot\|_{\mathbb{M}} \leq \sqrt{M}\|\cdot\|_{0,\Omega}$, we can easily see that

$$\|\boldsymbol{\xi} - \boldsymbol{\Pi}_2^{0,k_2}\boldsymbol{\xi}\|_{\mathbb{M}} \leq \sum_{E\in\mathcal{T}_h} \sqrt{M}\|\boldsymbol{\xi} - \boldsymbol{\Pi}_2^{0,k_2}\boldsymbol{\xi}\|_{0,E} \lesssim \sum_{E\in\mathcal{T}_h} h_E^{s_2+1}\sqrt{M}|\boldsymbol{\xi}|_{s_2+1,E} \leq h^{s_2+1}|\boldsymbol{\xi}|_{s_2+1,\mathbf{V}_2},$$
$$\|\psi - \Pi_2^{0,k_2}\psi\|_{Q_{b_2}} = \sum_{E\in\mathcal{T}_h} \frac{1}{\sqrt{M}}\|\psi - \Pi_2^{0,k_2}\psi\|_{0,E} \lesssim \sum_{E\in\mathcal{T}_h} h_E^{s_2+1}\frac{1}{\sqrt{M}}|\psi|_{s_2+1,E} \leq h^{s_2+1}|\psi|_{s_2+1,Q_{b_2}}. \qquad \square$$

Interpolation. The Fortin operator $\boldsymbol{\Pi}_2^{F,k_2} : \mathbf{H}^1(E) \to \mathbf{V}_2^{h,k_2}(E)$ can be defined directly from (4.9) as

$$\mathrm{dof}_j(\boldsymbol{\xi} - \boldsymbol{\Pi}_2^{F,k_2}\boldsymbol{\xi}) = 0, \quad \text{for all } j = 1, \dots, \dim(\mathbf{V}_2^{h,k_2}(E)) \text{ and for } \boldsymbol{\xi} \in \mathbf{H}^1(E).$$

Moreover, (4.9b) and an integration by parts imply the following commutative property:

$$\operatorname{div} \boldsymbol{\Pi}_2^{F,k_2}\boldsymbol{\xi} = \Pi_2^{0,k_2} \operatorname{div} \boldsymbol{\xi}.$$

Lemma 4.4. *The Fortin interpolation operator $\boldsymbol{\Pi}_2^{F,k_2}$ satisfies the following estimate*

$$\|\boldsymbol{\xi} - \boldsymbol{\Pi}_1^{F,k_2}\boldsymbol{\xi}\|_{\mathbb{M}} \lesssim h^{s_2+1}|\boldsymbol{\xi}|_{s_2+1,\mathbf{V}_2} \qquad \forall \boldsymbol{\xi} \in (\mathbf{H}^{s_2+1}(\Omega) \cap \mathbf{V}_2, |\cdot|_{s_2+1,\Omega}). \tag{4.11}$$

Proof. The standard interpolation estimate from [3] shows $\|\boldsymbol{\xi} - \boldsymbol{\Pi}_1^{F,k_2}\boldsymbol{\xi}\|_{0,E} \lesssim h^{s_2+1}|\boldsymbol{\xi}|_{s_2+1,E}$. Hence

$$\|\boldsymbol{\xi} - \boldsymbol{\Pi}_1^{F,k_2}\boldsymbol{\xi}\|_{\mathbb{M}} \leq \sum_{E\in\mathcal{T}_h} \sqrt{M}\|\boldsymbol{\xi} - \boldsymbol{\Pi}_1^{F,k_2}\boldsymbol{\xi}\|_{0,E} \lesssim \sum_{E\in\mathcal{T}_h} h^{s_2+1}\sqrt{M}|\boldsymbol{\xi}|_{s_2+1,E} \leq h^{s_2+1}|\boldsymbol{\xi}|_{s_2+1,\mathbf{V}_2}. \qquad \square$$

Discrete forms. Given $\boldsymbol{w}_h \in \mathbf{V}_1^{h,k_1}$ and $\tilde{r}_h \in Q_1^{h,k_1}$, let $a_2^{\boldsymbol{w}_h,\tilde{r}_h,E}(\cdot,\cdot)$ be the restriction of $a_2^{\boldsymbol{w}_h,\tilde{r}_h}(\cdot,\cdot)$ to E for $E \in \mathcal{T}_h$. Then

$$a_2^{\boldsymbol{w}_h,\tilde{r}_h,h,E}(\boldsymbol{\zeta}_h,\boldsymbol{\xi}_h) := a_2^{\boldsymbol{w}_h,\tilde{r}_h,E}(\boldsymbol{\Pi}_2^{0,k_2}\boldsymbol{\zeta}_h, \boldsymbol{\Pi}_2^{0,k_2}\boldsymbol{\xi}_h) + S_2^E(\boldsymbol{\zeta}_h - \boldsymbol{\Pi}_2^{0,k_2}\boldsymbol{\zeta}_h, \boldsymbol{\xi}_h - \boldsymbol{\Pi}_2^{0,k_2}\boldsymbol{\xi}_h),$$

where $S_2^E(\cdot,\cdot)$ is any symmetric and positive definite bilinear form defined on $\mathbf{V}_2^{h,k_2}(E) \times \mathbf{V}_2^{h,k_2}(E)$ that scales like $a_2^{\boldsymbol{w}_h,\tilde{r}_h,E}(\cdot,\cdot)$. In particular,

$$a_2^{\boldsymbol{w}_h,\tilde{r}_h,E}(\boldsymbol{\xi}_h,\boldsymbol{\xi}_h) \lesssim S_2^E(\boldsymbol{\xi}_h,\boldsymbol{\xi}_h) \lesssim a_2^{\boldsymbol{w}_h,\tilde{r}_h,E}(\boldsymbol{\xi}_h,\boldsymbol{\xi}_h), \quad \forall \boldsymbol{\xi}_h \in \ker(\boldsymbol{\Pi}_2^{0,k_2}). \tag{4.12}$$

The global discrete bilinear form is defined as

$$a_2^{\boldsymbol{w}_h,\tilde{r}_h,h}(\boldsymbol{\zeta}_h,\boldsymbol{\xi}_h) = \sum_{E\in\mathcal{T}_h} a_2^{\boldsymbol{w}_h,\tilde{r}_h,h,E}(\boldsymbol{\zeta}_h,\boldsymbol{\xi}_h) \quad \forall \boldsymbol{\zeta}_h,\boldsymbol{\xi}_h \in \mathbf{V}_2^{h,k_2}.$$

Finally, the definition of $\mathbf{V}_2^{h,k_2}$ and Q_2^{h,k_2} allow us to extend the bilinear forms $b_2(\cdot,\cdot)$, $c_2(\cdot,\cdot)$ and the linear forms $F_1(\cdot)$, $G_2(\cdot)$ to computable discrete bilinear forms as follows

$$b_2^h(\boldsymbol{\xi}_h,\varphi_h) = \sum_{E\in\mathcal{T}_h} \int_E \varphi_h \operatorname{div} \boldsymbol{\xi}_h = b_2(\boldsymbol{\xi}_h,\varphi_h), \quad c_2^h(\varphi_h,\psi_h) = \sum_{E\in\mathcal{T}_h} \int_E \varphi_h\psi_h = c_2(\varphi_h,\psi_h),$$

$$F_2^h(\boldsymbol{\xi}_h) = \sum_{E\in\mathcal{T}_h} \langle \varphi_D, \boldsymbol{\xi}_h \cdot \boldsymbol{n}\rangle_{\partial E\cap\Gamma_D} = F_2(\xi_h) \quad \text{and} \quad G_2^h(\psi_h) = \sum_{E\in\mathcal{T}_h} \int_E g\psi_h = G_2(\psi_h),$$

where a proper order in the quadrature rule is used for φ_D and g in $F_2(\boldsymbol{\xi})$ and $G_2(\psi_h)$, respectively.

Discrete formulation. Given $\boldsymbol{w}_h \in \mathbf{V}_1^{h,k_1}$ and $\tilde{r}_h \in Q_1^{h,k_1}$, find $(\boldsymbol{\zeta}_h,\varphi_h) \in \mathbf{V}_2^{h,k_2} \times Q_2^{h,k_2}$ such that

$$a_2^{\boldsymbol{w}_h,\tilde{r}_h,h}(\boldsymbol{\zeta}_h,\boldsymbol{\xi}_h) + b_2(\boldsymbol{\xi}_h,\varphi_h) = F_2(\boldsymbol{\xi}_h) \qquad \forall \boldsymbol{\xi}_h \in \mathbf{V}_2^{h,k_2}, \tag{4.13a}$$

$$b_2(\boldsymbol{\zeta}_h,\psi_h) - \theta c_2(\varphi_h,\psi_h) = G_2(\psi_h) \qquad \forall \psi_h \in Q_2^{h,k_2}. \tag{4.13b}$$

4.3. Well-posedness analysis of the discrete problem. Let us recall an abstract result from [7, Lemma 5.1] which adapts Theorem 3.1 to the discrete setting.

Theorem 4.5. *Let $V^h \subset V, Q_b^h \subset Q$ be Hilbert spaces endowed with the norms $\|\cdot\|_{V^h}$ and $\|\cdot\|_{Q_b^h}$, let Q^h be a dense (with respect to the norm $\|\cdot\|_{Q_b^h}$) linear subspace of Q_b^h and three bilinear forms $a^h(\cdot,\cdot)$ on $V^h \times V^h$ (continuous, symmetric and positive semi-definite), $b^h(\cdot,\cdot)$ on $V^h \times Q_b^h$ (continuous), and $c^h(\cdot,\cdot)$ on $Q^h \times Q^h$ (symmetric and positive semi-definite); which define three linear operators $A^h : V^h \to (V^h)'$, $B^h : V^h \to (Q_b^h)'$ and $C^h : Q^h \to (Q^h)'$, respectively. Suppose further that*

$$\|\hat{v}_h\|_{V^h}^2 \lesssim a^h(\hat{v}_h,\hat{v}_h) \qquad \forall \hat{v}_h \in \operatorname{Ker}(B^h), \tag{4.14a}$$

$$\|q_h\|_{Q_b^h} \lesssim \sup_{v_h\in V^h} \frac{b^h(v_h,q_h)}{\|v_h\|_{V^h}} \qquad \forall q_h \in Q_b^h. \tag{4.14b}$$

Assume that Q^h is complete with respect to the norm $\|\cdot\|^2_{Q^h} := \|\cdot\|^2_{Q^h_b} + t^2|\cdot|^2_{c^h}$, where $|\cdot|^2_{c^h} := c^h(\cdot,\cdot)$ is a semi-norm in Q^h. Let $t \in [0,1]$ and set the parameter-dependent energy norm as

$$\|(v_h, q_h)\|^2_{V^h\times Q^h} := \|v_h\|^2_{V^h} + \|q_h\|^2_{Q^h} = \|v_h\|^2_{V^h} + \|q_h\|^2_{Q^h_b} + t^2|q|^2_{c^h}.$$

Assume also that the following inf-sup condition holds

$$\|u_h\|_{V^h} \lesssim \sup_{(v_h,q_h)\in V^h\times Q^h} \frac{a^h(u_h,v_h) + b^h(v_h,q_h)}{\|(v_h,q_h)\|_{V^h\times Q^h}} \qquad \forall u_h \in V^h. \tag{4.15}$$

Then, for every $F^h \in (V^h)'$ and $G^h \in (Q^h)'$, there exists a unique $(u_h,p_h) \in V^h \times Q^h$ satisfying

$$\begin{aligned} a^h(u_h,v_h) + b^h(v_h,p_h) &= F^h(v_h) \qquad \forall v_h \in V^h,\\ b^h(u_h,q_h) - t^2c^h(p_h,q_h) &= G^h(q_h) \qquad \forall q_h \in Q^h. \end{aligned}$$

Furthermore, the following continuous dependence on data holds

$$\|(u_h,p_h)\|_{V^h\times Q^h} \lesssim \|F^h\|_{(V^h)'} + \|G^h\|_{(Q^h)'}. \tag{4.17}$$

The well-posedness of the uncoupled discrete problems (4.7) and (4.13) is given next.

Lemma 4.6. *Given $\vartheta_h \in Q_2^{h,k_2}$, assume that $1 \le \lambda$ and $0 < \mu$. Then, there exists a unique pair $(\boldsymbol{u}_h, \tilde{p}_h) \in \mathbf{V}_1^{h,k_1} \times Q_1^{h,k_1}$ solution to (4.7).*

Proof. The same arguments in Lemma 3.2 can be used to carry over the properties of $c_1(\cdot,\cdot)$ and $G_1^{\vartheta_h}(\cdot)$ to the discrete formulation. On the other hand, the positive semi-definiteness of the stabilisation term $S_1^E(\cdot,\cdot)$ allows us to extend the properties of $a_1(\cdot,\cdot)$ to the discrete operator $a_1^h(\cdot,\cdot)$. Concerning boundedness, the second inequality in (4.6) leads for all $\boldsymbol{u}_h \in \mathbf{V}_1^{h,k_1}(E)$ to

$$a_1^{h,E}(\boldsymbol{u}_h,\boldsymbol{u}_h) \lesssim a_1^E(\boldsymbol{\Pi}_1^{\boldsymbol{\varepsilon},k_1}\boldsymbol{u}_h, \boldsymbol{\Pi}_1^{\boldsymbol{\varepsilon},k_1}\boldsymbol{u}_h) + a_1^E(\boldsymbol{u}_h - \boldsymbol{\Pi}_1^{\boldsymbol{\varepsilon},k_1}\boldsymbol{u}_h, \boldsymbol{u}_h - \boldsymbol{\Pi}_1^{\boldsymbol{\varepsilon},k_1}\boldsymbol{u}_h) = \|\boldsymbol{u}_h\|^2_{\mathbf{V}_1(E)}.$$

This and the Cauchy–Schwarz inequality for the inner product show that

$$a_1^{h,E}(\boldsymbol{u}_h,\boldsymbol{v}_h) \le \sqrt{a_1^{h,E}(\boldsymbol{u}_h,\boldsymbol{u}_h)}\sqrt{a_1^{h,E}(\boldsymbol{v}_h,\boldsymbol{v}_h)} \lesssim \|\boldsymbol{u}_h\|_{\mathbf{V}_1(E)}\|\boldsymbol{v}_h\|_{\mathbf{V}_1(E)} \qquad \forall \boldsymbol{u}_h,\boldsymbol{v}_h \in \mathbf{V}_1^{h,k_1}.$$

Regarding the first Brezzi condition (4.14a), the first inequality in (4.6) gives

$$\|\boldsymbol{v}_h\|^2_{\mathbf{V}_1(E)} = a_1^E(\boldsymbol{\Pi}_1^{\boldsymbol{\varepsilon},k_1}\boldsymbol{v}_h, \boldsymbol{\Pi}_1^{\boldsymbol{\varepsilon},k_1}\boldsymbol{v}_h) + a_1^E(\boldsymbol{v}_h - \boldsymbol{\Pi}_1^{\boldsymbol{\varepsilon},k_1}\boldsymbol{v}_h, \boldsymbol{v}_h - \boldsymbol{\Pi}_1^{\boldsymbol{\varepsilon},k_1}\boldsymbol{v}_h) \lesssim a_1^{h,E}(\boldsymbol{v}_h,\boldsymbol{v}_h) \quad \forall \boldsymbol{v}_h \in \mathbf{V}_1^{h,k_1}(E).$$

Next, thanks to [4, Proposition 4.2] we can state the following discrete inf-sup condition

$$\|\tilde{q}_h\|_{0,\Omega} \lesssim \sup_{\boldsymbol{v}_h\in\mathbf{V}_1^{h,k_1}} \frac{b_1(\boldsymbol{v}_h,\tilde{q}_h)}{\|\nabla\boldsymbol{v}_h\|_{0,\Omega}} \qquad \forall \tilde{q}_h \in Q_1^{h,k_1}.$$

And with an analogous argument as in the second part of the proof of Lemma 3.2, we can show that the second discrete Brezzi condition (4.14b) holds

$$\|\tilde{q}_h\|_{Q_{b_1}} \lesssim \sup_{\boldsymbol{v}_h\in\mathbf{V}_1^{h,k_1}} \frac{b_1(\boldsymbol{v}_h,\tilde{q}_h)}{\|\boldsymbol{v}_h\|_{\mathbf{V}_1}} \qquad \forall \tilde{q}_h \in Q_1^{h,k_1}.$$

The continuity of $F^h(\cdot)$ can be obtained directly from the Cauchy–Schwarz inequality and the boundedness of $\boldsymbol{\Pi}^{0,k_1-2}$. Finally, for $\boldsymbol{u}_h \in \mathbf{V}_1^{h,k_1}$, we set $\boldsymbol{v}_h = \boldsymbol{u}_h$ and $\tilde{q}_h = 0$. Then, (4.14a) leads to

$$\|\boldsymbol{u}_h\|^2_{\mathbf{V}_1} \lesssim a_1^h(\boldsymbol{u}_h,\boldsymbol{u}_h) = a_1^h(\boldsymbol{u}_h,\boldsymbol{u}_h) + b_1(\boldsymbol{u}_h,0) \text{ and } \|(\boldsymbol{u}_h,0)\|^2_{\mathbf{V}_1\times Q_1} = \|\boldsymbol{u}_h\|^2_{\mathbf{V}_1}.$$

This proves that

$$\|\boldsymbol{u}_h\|_{\mathbf{V}_1} \lesssim \sup_{(\boldsymbol{v}_h,\tilde{q}_h)\in\mathbf{V}_1^{h,k_1}\times Q_1^{h,k_1}} \frac{a_1^h(u_h,v_h) + b_1(v_h,\tilde{q}_h)}{\|(\boldsymbol{v}_h,\tilde{q}_h)\|_{\mathbf{V}_1\times Q_1}} \quad \forall \boldsymbol{u}_h \in \mathbf{V}_1^{h,k_1}.$$

Therefore, the conditions of Theorem 4.5 are verified and we also obtain

$$\|(\boldsymbol{u}_h,\tilde{p}_h)\|_{\mathbf{V}_1\times Q_1} \le \overline{C}_1\left(\|F_1^h\|_{\mathbf{V}_1'} + \|G_1^{\vartheta_h}\|_{Q_1'}\right), \tag{4.18}$$

where the constant $\overline{C}_1 > 0$ does not depend on h and the physical parameters. □

LEMMA 4.7. *For a fixed pair* $(\boldsymbol{w}_h, \tilde{r}_h) \in \mathbf{V}_1^{h,k_1} \times Q_1^{h,k_1}$*, assume that* $0 \le \theta \le \frac{1}{M} \le 1$*. Then, there exists a unique pair* $(\boldsymbol{\xi}_h, \varphi_h) \in \mathbf{V}_2^{h,k_2} \times Q_2^{h,k_2}$ *solution to* (4.13).

Proof. Since $c_2(\cdot,\cdot)$, $F_2(\cdot)$ and $G_2(\cdot)$ remain same in the discrete formulation, the analogous arguments as in Lemma 3.3 will hold. The second stability inequality in (4.12) leads for all $\boldsymbol{\zeta}_h \in \mathbf{V}_2^{h,k_2}(E)$ to

$$a_2^{\boldsymbol{w}_h,\tilde{r}_h,h,E}(\boldsymbol{\zeta}_h,\boldsymbol{\zeta}_h) \lesssim a_2^{\boldsymbol{w}_h,\tilde{r}_h,E}(\boldsymbol{\Pi}_2^{0,k_2}\boldsymbol{\zeta}_h, \boldsymbol{\Pi}_2^{0,k_2}\boldsymbol{\zeta}_h) + a_2^{\boldsymbol{w}_h,\tilde{r}_h,E}(\boldsymbol{\zeta}_h - \boldsymbol{\Pi}_2^{0,k_2}\boldsymbol{\zeta}_h, \boldsymbol{\zeta}_h - \boldsymbol{\Pi}_2^{0,k_2}\boldsymbol{\zeta}_h) \le \|\boldsymbol{\zeta}_h\|_{\mathbf{V}_2(E)}^2.$$

For all $\boldsymbol{\zeta}_h, \boldsymbol{\xi}_h \in \mathbf{V}_2^{h,k_2}$, this results in

$$a_2^{\boldsymbol{w}_h,\tilde{r}_h,h,E}(\boldsymbol{\zeta}_h,\boldsymbol{\xi}_h) \le \sqrt{a_2^{\boldsymbol{w}_h,\tilde{r}_h,h,E}(\boldsymbol{\zeta}_h,\boldsymbol{\zeta}_h)}\sqrt{a_2^{\boldsymbol{w}_h,\tilde{r}_h,h,E}(\boldsymbol{\xi}_h,\boldsymbol{\xi}_h)} \lesssim \|\boldsymbol{\zeta}_h\|_{\mathbf{V}_2(E)}\|\boldsymbol{\xi}_h\|_{\mathbf{V}_2(E)}.$$

Hence $a_2^{\boldsymbol{w}_h,\tilde{r}_h,h}(\cdot,\cdot)$ is a bounded operator. For condition (4.14a), note that $\mathrm{Ker}(B_2^h(E)) = \{\boldsymbol{\xi}_h \in \mathbf{V}_2^{h,k_2}(E) : \int_E \varphi_h \operatorname{div}\boldsymbol{\xi}_h = 0\} \subseteq \mathrm{Ker}(B_2)$ which together with the first inequality in (4.12) imply that

$$\begin{aligned}\|\hat{\boldsymbol{\xi}}_h\|_{\mathbf{V}_2(E)}^2 &= a_2^{\boldsymbol{w}_h,\tilde{r}_h,E}(\hat{\boldsymbol{\xi}}_h,\hat{\boldsymbol{\xi}}_h) + a_2^{\boldsymbol{w}_h,\tilde{r}_h,E}(\hat{\boldsymbol{\xi}}_h - \boldsymbol{\Pi}_2^{0,k_2}\hat{\boldsymbol{\xi}}_h, \hat{\boldsymbol{\xi}}_h - \boldsymbol{\Pi}_2^{0,k_2}\hat{\boldsymbol{\xi}}_h)\\ &\lesssim a_2^{\boldsymbol{w}_h,\tilde{r}_h,h,E}(\hat{\boldsymbol{\xi}}_h,\hat{\boldsymbol{\xi}}_h) \qquad \forall \hat{\boldsymbol{\xi}}_h \in \mathrm{Ker}(B_2^h(E)).\end{aligned}$$

The Fortin operator defined in Section 4.2 leads to a discrete inf-sup condition in the non-weighted norms. Proceeding as in Lemma 3.3, the second discrete Brezzi condition (4.14b) reads

$$\|\varphi_h\|_{Q_{b_2}} \lesssim \sup_{\boldsymbol{\zeta}\in\mathbf{V}_2^{h,k_2}} \frac{b_2(\boldsymbol{\zeta}_h,\varphi_h)}{\|\boldsymbol{\zeta}_h\|_{\mathbf{V}_2}} \qquad \forall \varphi_h \in Q_2^{h,k_2}.$$

Finally, (4.15) is deduced as follows: for $\boldsymbol{\zeta}_h \in \mathbf{V}_2^{h,k_2}$, take $\boldsymbol{\xi}_h = \boldsymbol{\zeta}_h$ and $\varphi_h = M\operatorname{div}\boldsymbol{\zeta}_h$ to obtain

$$\|\boldsymbol{\zeta}_h\|_{\mathbf{V}_2}^2 = a_2^{\boldsymbol{w}_h,\tilde{r}_h}(\boldsymbol{\zeta}_h,\boldsymbol{\zeta}_h) + Mb_2(\boldsymbol{\zeta}_h,\operatorname{div}\boldsymbol{\zeta}_h) \lesssim a_2^{\boldsymbol{w}_h,\tilde{r}_h,h}(\boldsymbol{\zeta}_h,\boldsymbol{\zeta}_h) + b_2(\boldsymbol{\zeta}_h, M\operatorname{div}\boldsymbol{\zeta}_h),$$

and

$$\begin{aligned}\|(\boldsymbol{\zeta}_h, M\operatorname{div}\boldsymbol{\zeta}_h)\|_{\mathbf{V}_2\times Q_2}^2 &= \|\boldsymbol{\zeta}_h\|_{\mathbf{V}_2}^2 + \|M\operatorname{div}\zeta_h\|_{Q_{b_2}}^2 + \theta|M\operatorname{div}\boldsymbol{\zeta}_h|_{c_2}^2\\ &\lesssim \|\boldsymbol{\zeta}_h\|_{\mathbf{V}_2}^2 + \frac{1}{M}\|M\operatorname{div}\boldsymbol{\zeta}_h\|_{0,\Omega}^2 \lesssim \|\boldsymbol{\zeta}_h\|_{\mathbf{V}_2}^2.\end{aligned}$$

Therefore,

$$\|\boldsymbol{\zeta}_h\|_{\mathbf{V}_2} \lesssim \sup_{(\boldsymbol{\xi}_h,\varphi_h)\in\mathbf{V}_2^{h,k_2}\times Q_2^{h,k_2}} \frac{a_2^{\boldsymbol{w}_h,\tilde{r}_h,h}(\boldsymbol{\zeta}_h,\boldsymbol{\xi}_h) + b_2(\boldsymbol{\xi}_h,\varphi_h)}{\|(\boldsymbol{\xi}_h,\varphi_h)\|_{\mathbf{V}_2\times Q_2}} \quad \forall \boldsymbol{\zeta}_h \in \mathbf{V}_2^{h,k_2}.$$

This proves that the conditions of Theorem 4.5 hold. Furthermore, we have

$$\|(\boldsymbol{\zeta}_h,\varphi_h)\|_{\mathbf{V}_2\times Q_1} \le \overline{C}_2\left(\|F_2\|_{\mathbf{V}_2} + \|G_2\|_{Q_1}\right), \tag{4.19}$$

where the constant $\overline{C}_2 > 0$ does not depend on h and the physical parameters. ∎

We finish this subsection by introducing the full coupled discrete formulation. For given $\boldsymbol{f} \in \mathbf{L}^2(\Omega)$, $g \in L^2(\Omega)$, and $\varphi_D \in H^{\frac{1}{2}}(\Gamma_D)$, find $(\boldsymbol{u}_h, \tilde{p}_h, \boldsymbol{\zeta}_h, \varphi_h) \in \mathbf{V}_1^{h,k_1} \times Q_1^{h,k_1} \times \mathbf{V}_2^{h,k_2} \times Q_2^{h,k_2}$ such that

$$a_1^h(\boldsymbol{u}_h,\boldsymbol{v}_h) + b_1(\boldsymbol{v}_h,\tilde{p}_h) = F_2^h(\boldsymbol{v}_h) \qquad \forall \boldsymbol{v}_h \in \mathbf{V}_1^{h,k_1}, \tag{4.20a}$$

$$b_1(\boldsymbol{u}_h,\tilde{q}_h) - \frac{1}{\lambda}c_1(\tilde{p}_h,\tilde{q}_h) = G_1^{\varphi_h}(\tilde{q}_h) \qquad \forall \tilde{p}_h \in Q_1^{h,k_1}, \tag{4.20b}$$

$$a_2^{\boldsymbol{u}_h,\tilde{p}_h,h}(\boldsymbol{\zeta}_h,\boldsymbol{\xi}_h) + b_2(\boldsymbol{\xi}_h,\varphi_h) = F_2(\boldsymbol{\xi}_h) \qquad \forall \boldsymbol{\xi}_h \in \mathbf{V}_2^{h,k_2}, \tag{4.20c}$$

$$b_2(\boldsymbol{\zeta}_h,\psi_h) - \theta c_2(\varphi_h,\psi_h) = G_2(\psi_h) \qquad \forall \psi_h \in Q_2^{h,k_2}. \tag{4.20d}$$

4.4. Discrete fixed-point strategy. Following the approach in the continuous case, we define the discrete solution operators as follows

$$\mathcal{S}_1^h : Q_2^{h,k_2} \to \mathbf{V}_1^{h,k_1} \times Q_1^{h,k_1}, \quad \vartheta_h \mapsto \mathcal{S}_1^h(\vartheta_h) = (\mathcal{S}_{11}^h(\vartheta_h), \mathcal{S}_{12}^h(\vartheta_h)) := (\boldsymbol{u}_h, \tilde{p}_h),$$

where $(\boldsymbol{u}_h, \tilde{p}_h)$ is the unique solution to (4.7); and

$$\mathcal{S}_2^h : \mathbf{V}_1^{h,k_1} \times Q_1^{h,k_1} \to \mathbf{V}_2^{h,k_2} \times Q_2^{h,k_2}, \quad (\boldsymbol{w}_h, \tilde{r}_h) \mapsto \mathcal{S}_2^h(\boldsymbol{w}_h, \tilde{r}_h) = (\mathcal{S}_{21}^h(\boldsymbol{w}_h, \tilde{r}_h), \mathcal{S}_{22}^h(\boldsymbol{w}_h, \tilde{r}_h)) := (\boldsymbol{\zeta}_h, \varphi_h),$$

where $(\boldsymbol{\zeta}_h, \varphi_h)$ is the unique solution to (4.13). The discrete version of (2.6) is thus equivalent to the following discrete fixed-point equation:

$$\text{Find } \varphi_h \in Q_2^{h,k_2} \text{ such that } \mathcal{A}^h(\varphi_h) = \varphi_h,$$

where $\mathcal{A}^h : Q_2^{h,k_2} \to Q_2^{h,k_2}$ is defined as $\varphi_h \mapsto \mathcal{A}^h(\varphi_h) := (\mathcal{S}_{22}^h \circ \mathcal{S}_1^h)(\varphi_h)$.

Lemma 4.8. *The operator $\mathcal{S}_1^h$ is Lipschitz continuous with Lipschitz constant $L_{\mathcal{S}_1^h} = \sqrt{M}\overline{C}_1 L_\ell$.*

Proof. The result follows applying to Lemma 4.6 analogous arguments used to prove Lemma 3.4. ∎

Lemma 4.9. *The operator $\mathcal{S}_2^h$ is Lipschitz continuous with Lipschitz constant*

$$L_{\mathcal{S}_2^h} = \max\left\{\frac{1}{\sqrt{2\mu}}, \sqrt{2\mu}\right\}\sqrt{M^3}\overline{C}_2^2 L_{\mathbb{M}}\left(\|\varphi_D\|_{\frac{1}{2},\Gamma_D} + \|g\|_{0,\Omega}\right).$$

Proof. Similar techniques from Lemma 3.5 adapted to Lemma 4.7 conclude the proof. ∎

Lemma 4.10. *The operator $\mathcal{A}^h$ is Lipschitz continuous with Lipschitz constant $L_{\mathcal{A}^h} = L_{\mathcal{S}_2^h} L_{\mathcal{S}_1^h}$.*

Proof. It follows directly from Lemmas 4.8-4.9. ∎

Next, we define the set

$$\mathbf{W}^h = \left\{\boldsymbol{w}_h \in Q_2^{h,k_2} : \|w_h\|_{Q_2} \le \sqrt{M}\overline{C}_2\left(\|\varphi_D\|_{\frac{1}{2},\Gamma_D} + \|g\|_{0,\Omega}\right)\right\}, \tag{4.21}$$

which satisfies that $\mathcal{A}^h(\mathbf{W}^h) \subseteq \mathbf{W}^h$. Indeed, from (4.19), we readily see that

$$\|A^h(\varphi_h)\|_{Q_2} = \|S_{22}^h(S_1^h(\varphi_h))\|_{Q_2} \le \|S_2^h(S_1^h(\varphi_h))\|_{\mathbf{V}_2\times Q_2} \le \sqrt{M}\overline{C}_2\left(\|\varphi_D\|_{\frac{1}{2},\Gamma_D} + \|g\|_{0,\Omega}\right).$$

The following theorem provides the well-posedness of the discrete coupled problem.

Theorem 4.11. *Let $\mathbf{W}^h$ be as in (4.21) and assume that $L_{\mathcal{A}^h} < 1$. Then the operator $\mathcal{A}^h$ has a unique fixed point $\varphi_h \in \mathbf{W}^h$. Equivalently, the discrete coupled problem (4.20) has a unique solution $(\boldsymbol{u}_h, \tilde{p}_h, \boldsymbol{\zeta}_h, \varphi_h) \in \mathbf{V}_1^{h,k_1} \times Q_1^{h,k_1} \times \mathbf{V}_2^{h,k_2} \times Q_2^{h,k_2}$ and the following continuous dependence on data holds*

$$\|(\boldsymbol{u}_h, \tilde{p}_h)\|_{\mathbf{V}_1\times Q_1} \le \overline{C}_1\left(\|F_1^h\|_{\mathbf{V}_1'} + \|G_1^{\varphi_h}\|_{Q_1'}\right), \qquad \|(\boldsymbol{\zeta}_h, \varphi_h)\|_{\mathbf{V}_2\times Q_2} \le \overline{C}_2\left(\|F_2\|_{\mathbf{V}_2'} + \|G_2\|_{Q_2'}\right),$$

where the corresponding constants $\overline{C}_1$ and $\overline{C}_2$ do not depend on the physical parameters.

Proof. It follows readily from Lemma 4.10 together with the Banach fixed-point theorem. ∎

5. A priori error analysis.

In this section, we aim to provide the convergence of the VE discretisation developed in Section 4 and derive the corresponding convergence result which preserves the robustness proved in Theorem 3.1 and Theorem 4.5.

Lemma 5.1. *In addition to the assumptions of Theorems 3.7 and 4.11, let $(\boldsymbol{u}, \tilde{p}, \boldsymbol{\zeta}, \varphi) \in \mathbf{V}_1 \times Q_1 \times \mathbf{V}_2 \times Q_2$ and $(\boldsymbol{u}_h, \tilde{p}_h, \boldsymbol{\zeta}_h, \varphi_h) \in \mathbf{V}_1^{h,k_1} \times Q_1^{h,k_1} \times \mathbf{V}_2^{h,k_2} \times Q_2^{h,k_2}$ be the unique solutions to (2.6) and (4.20), respectively. Then the following estimates hold*

$$\begin{aligned}\|(\boldsymbol{u} - \boldsymbol{u}_h, \tilde{p} - \tilde{p}_h)\|_{\mathbf{V}_1\times Q_1} \lesssim\ & \|\boldsymbol{u} - \boldsymbol{\Pi}_1^{\boldsymbol{\varepsilon},k_1}\boldsymbol{u}\|_{\mathbf{V}_1^{h,k_1}} + \|\boldsymbol{u} - \boldsymbol{\Pi}_1^{F,k_1}\boldsymbol{u}\|_{\mathbf{V}_1} \\ & + \|F_1^h - F_1\|_{\mathbf{V}_1'} + \|\tilde{p} - \Pi_1^{0,k_1-1}\tilde{p}\|_{Q_{b_1}},\end{aligned} \tag{5.1a}$$

$$\|(\boldsymbol{\zeta} - \boldsymbol{\zeta}_h, \varphi - \varphi_h)\|_{\mathbf{V}_2\times Q_2} \lesssim \|\boldsymbol{\zeta} - \boldsymbol{\Pi}_2^{0,k_2}\boldsymbol{\zeta}\|_{\mathbb{M}} + \|\boldsymbol{\zeta} - \boldsymbol{\Pi}_2^{F,k_2}\boldsymbol{\zeta}\|_{\mathbf{V}_2} + \|\varphi - \Pi_2^{0,k_2}\varphi\|_{Q_{b_2}}, \tag{5.1b}$$

where the discrete norms are defined as $\|\cdot\|_{\mathbf{V}_1^{h,k_1}} = \sum_{E\in\mathcal{T}_h}\|\cdot\|_{\mathbf{V}_1^{h,k_1}(E)} = \sum_{E\in\mathcal{T}_h}\|\cdot\|_{\mathbf{V}_1(E)}$.

Proof. First we set the notation $\boldsymbol{u}_I = \boldsymbol{\Pi}_1^{F,k_1}\boldsymbol{u}$, $\boldsymbol{u}_\pi = \boldsymbol{\Pi}_1^{\boldsymbol{\varepsilon},k_1}\boldsymbol{u}$ and $\tilde{p}_\pi = \Pi_1^{0,k_1-1}\tilde{p}$. From (2.10) and (4.7) we can readily see that $(\boldsymbol{u}_h - \boldsymbol{u}_I, \tilde{p}_h - \tilde{p}_\pi) \in \mathbf{V}_1^{h,k_1} \times Q_1^{h,k_1}$ is the unique solution to

$$\begin{aligned}a_1^h(\boldsymbol{u}_h - \boldsymbol{u}_I, \boldsymbol{v}_h) + b_1(\boldsymbol{v}_h, \tilde{p}_h - \tilde{p}_\pi) &= \check{F}_1(\boldsymbol{v}_h) && \forall \boldsymbol{v}_h \in \mathbf{V}_1^{h,k_1}, \\ b_1(\boldsymbol{u}_h - \boldsymbol{u}_I, \tilde{q}_h) - \frac{1}{\lambda}c_1(\tilde{p}_h - \tilde{p}_\pi, \tilde{q}_h) &= \check{G}_1(\tilde{q}_h) && \forall \tilde{q}_h \in Q_1^{h,k_1},\end{aligned}$$

where

$$\check{F}_1(\boldsymbol{v}_h) = a_1(\boldsymbol{u}, \boldsymbol{v}_h) - a_1^h(\boldsymbol{u}_I, \boldsymbol{v}_h) + (F_1^h - F_1)(\boldsymbol{v}_h) - b_1(\boldsymbol{v}_h, \tilde{p}_\pi - \tilde{p}),$$

$$\check{G}_1(\tilde{q}_h) = -b_1(\boldsymbol{u}_I - \boldsymbol{u}, \tilde{q}_h) + \frac{1}{\lambda} c_1(\tilde{p}_\pi - \tilde{p}, \tilde{q}_h).$$

The continuous dependence on data (4.18) shows

$$\|(\boldsymbol{u}_h - \boldsymbol{u}_I, \tilde{p}_h - \tilde{p}_\pi)\|_{\mathbf{V}_1 \times Q_1} \lesssim \|\check{F}_1\|_{\mathbf{V}_1'} + \|\check{G}_1\|_{Q_1'}.$$

The continuity from Lemma 3.2 (resp. Lemma 4.6) for $a_1(\cdot,\cdot)$ and $b_1(\cdot,\cdot)$ (resp. $a_1^h(\cdot,\cdot)$) together with $a_1^h(\boldsymbol{u}_\pi, \boldsymbol{u}_h) = a_1(\boldsymbol{u}_\pi, \boldsymbol{u}_h)$ provide

$$\begin{aligned}
\|\check{F}_1\|_{\mathbf{V}_1'} &\lesssim \|\boldsymbol{u} - \boldsymbol{u}_\pi\|_{\mathbf{V}_1^{h,k_1}} + \|\boldsymbol{u}_\pi - \boldsymbol{u}_I\|_{\mathbf{V}_1^{h,k_1}} + \|F_1^h - F_1\|_{\mathbf{V}_1'} + \|\tilde{p} - \tilde{p}_\pi\|_{Q_{b_1}},\\
\|\check{G}_1\|_{Q_1'} &\lesssim \|\boldsymbol{u} - \boldsymbol{u}_I\|_{\mathbf{V}_1} + \|\tilde{p} - \tilde{p}_\pi\|_{Q_{b_1}}.
\end{aligned}$$

On the other hand, the triangle inequality leads to

$$\begin{gathered}
\|\boldsymbol{u} - \boldsymbol{u}_h\|_{\mathbf{V}_1} - \|\boldsymbol{u} - \boldsymbol{u}_I\|_{\mathbf{V}_1} \le \|\boldsymbol{u}_h - \boldsymbol{u}_I\|_{\mathbf{V}_1}, \quad \|\tilde{p} - \tilde{p}_h\|_{Q_{b_1}} - \|\tilde{p} - \tilde{p}_\pi\|_{Q_{b_1}} \le \|\tilde{p}_h - \tilde{p}_\pi\|_{Q_{b_1}},\\
\|\boldsymbol{u}_\pi - \boldsymbol{u}_I\|_{\mathbf{V}_1^{h,k_1}} \le \|\boldsymbol{u} - \boldsymbol{u}_I\|_{\mathbf{V}_1^{h,k_1}} + \|\boldsymbol{u} - \boldsymbol{u}_\pi\|_{\mathbf{V}_1^{h,k_1}}.
\end{gathered}$$

The combination of the estimates above proves (5.1a). For the second inequality, we adopt the notation $\boldsymbol{\zeta}_I = \boldsymbol{\Pi}_2^{F,k_2}\boldsymbol{\zeta}$, $\boldsymbol{\zeta}_\pi = \boldsymbol{\Pi}_2^{0,k_2}\boldsymbol{\zeta}$ and $\varphi_\pi = \Pi_2^{0,k_2}\varphi$. It is easy to check from (2.11) and (4.13) that $(\boldsymbol{\zeta}_h - \boldsymbol{\zeta}_I, \varphi_h - \varphi_\pi) \in \mathbf{V}_2^{h,k_2} \times Q_2^{h,k_2}$ is the unique solution to

$$\begin{aligned}
a_2^{\boldsymbol{w}_h,\tilde{r}_h,h}(\boldsymbol{\zeta}_h - \boldsymbol{\zeta}_I, \boldsymbol{\xi}_h) + b_2(\boldsymbol{\xi}_h, \varphi_h - \varphi_\pi) &= \check{F}_2(\boldsymbol{\xi}_h) \qquad \forall \boldsymbol{\xi}_h \in \mathbf{V}_2^{h,k_2},\\
b_2(\boldsymbol{\zeta}_h - \boldsymbol{\zeta}_I, \psi_h) - \theta c_2(\varphi_h - \varphi_\pi, \psi_h) &= \check{G}_2(\psi_h) \qquad \forall \psi_h \in Q_2^{h,k_2},
\end{aligned}$$

where

$$\begin{aligned}
\check{F}_2(\boldsymbol{\xi}_h) &= a_2^{\boldsymbol{w}_h,\tilde{r}_h}(\boldsymbol{\zeta}, \boldsymbol{\xi}_h) - a_2^{\boldsymbol{w}_h,\tilde{r}_h,h}(\boldsymbol{\zeta}_I, \boldsymbol{\xi}_h) - b_2(\boldsymbol{\xi}_h, \varphi_\pi - \varphi),\\
\check{G}_2(\psi_h) &= -b_2(\boldsymbol{\zeta}_I - \boldsymbol{\zeta}, \psi_h) + \theta c_2(\varphi_\pi - \varphi, \psi_h).
\end{aligned}$$

Owing to the continuous dependence on data (4.19) we arrive at

$$\|(\boldsymbol{\zeta}_h - \boldsymbol{\zeta}_I, \varphi_h - \varphi_\pi)\|_{\mathbf{V}_2 \times Q_2} \lesssim \|\check{F}_2(\boldsymbol{\xi}_h)\|_{\mathbf{V}_2'} + \|\check{G}_2(\psi_h)\|_{Q_2'}.$$

As a consequence of the continuity proved in Lemma 3.3 (resp. Lemma 4.7) for $b_2(\cdot,\cdot)$ (resp. $a_2^{\boldsymbol{w}_h,\tilde{r}_h,h}(\cdot,\cdot)$), in addition with $a_2^{\boldsymbol{w}_h,\tilde{r}_h,h}(\boldsymbol{\zeta}_\pi, \boldsymbol{\zeta}_h) = a_2^{\boldsymbol{w}_h,\tilde{r}_h}(\boldsymbol{\zeta}_\pi, \boldsymbol{\zeta}_h)$, we readily see that

$$\begin{aligned}
\|\check{F}_2(\boldsymbol{\xi}_h)\|_{\mathbf{V}_2'} &\lesssim \|\boldsymbol{\zeta} - \boldsymbol{\zeta}_\pi\|_{\mathbb{M}} + \|\boldsymbol{\zeta}_\pi - \boldsymbol{\zeta}_I\|_{\mathbb{M}} + \|\varphi - \varphi_\pi\|_{Q_{b_2}},\\
\|\check{G}_2(\psi_h)\|_{Q_2'} &\lesssim \|\boldsymbol{\zeta} - \boldsymbol{\zeta}_I\|_{\mathbf{V}_2} + \|\psi - \psi_\pi\|_{Q_{b_2}}.
\end{aligned}$$

Then, as before, it suffices to apply triangle inequality properly, allowing us to assert (5.1b). ∎

THEOREM 5.2. *Adopt the assumptions of Lemma 5.1. Assume further that* $(\boldsymbol{u}, \tilde{p}, \boldsymbol{\zeta}, \varphi) \in (\mathbf{H}^{s_1+1}(\Omega) \cap \mathbf{V}_1, |\cdot|_{s_1+1,\mathbf{V}_1}) \times (H^{s_1}(\Omega) \cap Q_{b_1}, |\cdot|_{s_1,Q_{b_1}}) \times (\mathbf{H}^{s_2+1} \cap \mathbf{V}_2, |\cdot|_{s_2+1,\mathbf{V}_2}) \times (H^{s_2+1} \cap Q_{b_2}, |\cdot|_{s_2+1,Q_{b_2}})$, $\boldsymbol{f} \in (\mathbf{H}^{s_1-1} \cap \mathbf{Q}_{b_1}, |\cdot|_{s_1-1,\mathbf{Q}_{b_1}})$ *and* $g \in (H^{s_2+1}(\Omega) \cap Q_{b_2}, |\cdot|_{s_2+1,Q_{b_2}})$ *with* $0 < s_1 \le k_1$ *and* $0 \le s_2 \le k_2$. *Then*

$$\|(\boldsymbol{u} - \boldsymbol{u}_h, \tilde{p} - \tilde{p}_h)\|_{\mathbf{V}_1 \times Q_1} \lesssim h^{s_1}(|\boldsymbol{f}|_{s_1-1,\mathbf{Q}_{b_1}} + |\boldsymbol{u}|_{s_1+1,\mathbf{V}_1} + |\tilde{p}|_{s_1,Q_{b_1}}), \tag{5.2a}$$

$$\|(\boldsymbol{\zeta} - \boldsymbol{\zeta}_h, \varphi - \varphi_h)\|_{\mathbf{V}_2 \times Q_2} \lesssim h^{s_2+1}(|g|_{s_2+1,Q_{b_2}} + |\boldsymbol{\zeta}|_{s_2+1,\mathbf{V}_2} + |\varphi|_{s_2+1,Q_{b_2}}). \tag{5.2b}$$

Proof. (5.2a) follows directly from (5.1a) together with Lemma 4.3, Lemma 4.2 and the following estimate (see [4, Lemma 3.2])

$$|(F_1^{h,E} - F_1^E)(\boldsymbol{v}_h)| \lesssim h_E^{s_1}|\boldsymbol{f}|_{s_1-1,E}|\boldsymbol{v}_h|_{1,E},$$

which leads to

$$|(F_1^h - F_1)(\boldsymbol{v}_h)| \le \sum_{E \in \mathcal{T}_h} |(F_1^{h,E} - F_1^E)(\boldsymbol{v}_h)| \lesssim \sum_{E \in \mathcal{T}_h} h_E^{s_1}|\boldsymbol{f}|_{s_1-1,E}|\boldsymbol{v}_h|_{1,E} \lesssim h^{s_1}|\boldsymbol{f}|_{s_1-1,\mathbf{Q}_{b_1}}\|\boldsymbol{v}_h\|_{\mathbf{V}_1}.$$

On the other hand, note that

$$\begin{aligned}
\sqrt{M}\|\operatorname{div}\boldsymbol{\zeta} - \operatorname{div}\boldsymbol{\Pi}_2^{F,k_2}\boldsymbol{\zeta}\|_{0,\Omega} &= \sqrt{M}\|\operatorname{div}\boldsymbol{\zeta} - \Pi_2^{0,k_2}\operatorname{div}\boldsymbol{\zeta}\|_{0,\Omega}\\
&= \sqrt{M}\|(g - \theta\varphi) - \Pi_2^{0,k_2}(g - \theta\varphi)\|_{0,\Omega} \lesssim h^{s_2+1}(|g|_{s_2+1,Q_{b_2}} + |\varphi|_{s_2+1,Q_{b_2}}).
\end{aligned}$$

Finally, (5.1b) in addition with Lemma 4.3 and Lemma 4.11 conclude the proof of (5.2b). ∎

6. Numerical tests. First, we verify the theoretical convergence rates proved in Section 5 with different polygonal meshes and polynomial orders (to be specified in Section 6.1). Next, we evaluate the robustness provided in Theorem 4.11 for different physical parameters (to be specified in Section 6.2). The numerical implementation is done with in-house MATLAB routines based on [32, 36]. We implemented (4.7) and (4.13) separately for $k_1 = 2$ and $k_2 = 0, 1$ respectively. The nonlinear coupled problem (4.20) is solved with a Picard iteration, following the same structure as in the fixed-point analysis from Section 4.4. The fixed-point tolerance is set to 10^{-8} and the errors are calculated as follows

$$\mathrm{e}_1(\boldsymbol{u} - \boldsymbol{u}_h, \tilde{p} - \tilde{p}_h) = \|(\boldsymbol{u} - \boldsymbol{\Pi}_1^{\boldsymbol{\varepsilon},k_1}\boldsymbol{u}_h, \tilde{p} - \Pi_1^{0,k_1-1}\tilde{p}_h)\|_{\mathbf{V}_1^{h,k_1}\times Q_1^{h,k_1}},$$
$$\mathrm{e}_2(\boldsymbol{\zeta} - \boldsymbol{\zeta}_h, \varphi - \varphi_h) = \|(\boldsymbol{\zeta} - \boldsymbol{\Pi}_2^{0,k_2}\boldsymbol{\zeta}_h, \varphi - \Pi_2^{0,k_2}\varphi_h)\|_{\mathbf{V}_2^{h,k_2}\times Q_2^{h,k_2}}.$$

The linear systems arising from the VE discretisation are solved using a direct solver. For the initial guess $\varphi_0 \in Q_2^{h,k_2}$, the scaled monomial basis introduced in Section 4 leads to $\varphi_0 = \mathbf{c}\cdot(1)$ and $\varphi_0 = \mathbf{c}\cdot(1, \frac{x-x_E}{h_E}, \frac{y-y_E}{h_E})$ for $k_1 = 0, 1$ respectively and $\mathbf{c}$ a constant vector of the appropriate size.

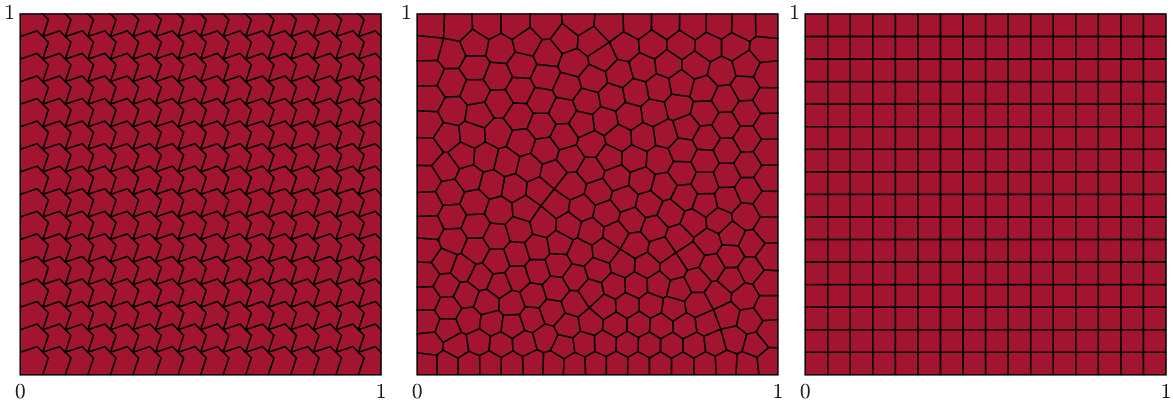

(a) Non–convex mesh. (b) Smooth Voronoi mesh. (c) Square mesh.

Fig. 6.1. *An illustration of three distinct coarse meshes each one consisting of 256 elements.*

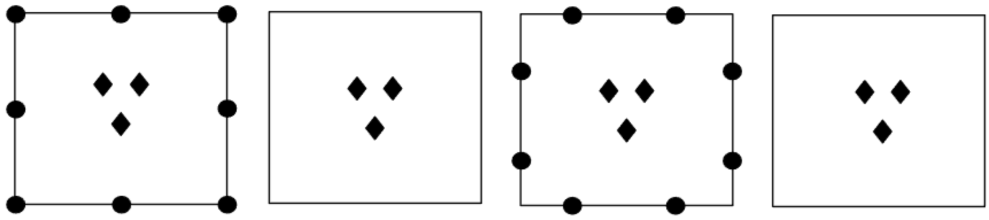
(a) DoFs for $\mathbf{V}_1^{h,2}$ (b) DoFs for $Q_1^{h,2}$ (c) DoFs for $\mathbf{V}_2^{h,1}$ (d) DoFs for $Q_2^{h,1}$

Fig. 6.2. *Illustration of the DoFs on a square element with $k_1 = 2$ and $k_2 = 1$.*

6.1. Example 1: Convergence test with smooth solution. This test is designed with the following manufactured solutions

$$\boldsymbol{u}(x,y) = \frac{1}{5}\left(\cos(x)\sin(y)x + x^2, \sin(x)\cos(y)x + y^2\right)^{\mathtt{t}}, \quad \varphi(x,y) = x^2 + y^2 + \sin^2(\pi x) + \cos^2(\pi y),$$

on $\Omega = (0,1)^2$ with Dirichlet part $\Gamma_D = \{(x,y) \in \partial\Omega \colon x = 0 \text{ or } y = 0\}$ and Neumann part $\Gamma_N = \partial\Omega \setminus \Gamma_D$. The exact displacement and concentration are used to compute exact Herrmann pressure $\tilde{p}$ and total flux $\boldsymbol{\zeta}$, as well as appropriate forcing term, source, and non-homogeneous traction, displacement, and flux boundary data. The nonlinear terms are taken in the form

$$\mathbb{M}(\boldsymbol{\sigma}) = m_0\exp(-m_1\operatorname{tr}\boldsymbol{\sigma})\mathbb{I}, \quad \ell(\vartheta) = K_0 + \frac{\vartheta^n}{K_1 + \vartheta^n},$$

with the arbitrary parameters (dimensionless in this case)

$$\lambda = 10^3, \quad \mu = 10^2, \quad \theta = 10^{-3}, \quad m_0 = 10^{-1}, \quad m_1 = 10^{-4}, \quad K_0 = 1, \quad K_1 = 1, \quad n = 2.$$

For the remaining parameter M, we use the `fmincom` MATLAB optimisation subroutine to compute

$$M = \max_{(x,y)\in\Omega} \quad \|\mathbb{M}(\sigma)\|_F = 1.157701 \times 10^1,$$

with $\|\cdot\|_F$ denoting the Frobenius matrix norm.

The performance of the VEM is verified on three different types of meshes: non-convex, voronoi, and square meshes (see Figure 6.1), and we consider a sequence of four successive refinements with 16, 64, 256, and 400 elements, ensuring consistency across the evaluations. As an illustrative example, the DoFs for a single square element are shown in Figure 6.2 for $k_1 = 2$ and $k_2 = 0, 1$. It is easy to check that the total number of DoFs for the spaces in Section 4 are given by $\mathrm{DOF}_1^j(k_1 = 2) = 3N_E^j + 2N_e^j + 2N_v^j + 3N_E^j$, $\mathrm{DOF}_2^j(k_2 = 0) = N_e^j + N_E^j$ and $\mathrm{DOF}_2^j(k_2 = 1) = 3N_E^j + 2N_e^j + 3N_E^j$, with N_E^j (resp. N_e^j, N_v^j) corresponding to the number of elements in the mesh j (resp. edges, vertices). Besides, the experimental order of convergence r_i for the error e_i of the refinement $j+1$ is computed from the formula

$$r_i^{j+1} = \frac{\log(\frac{\mathrm{e}_i^{j+1}}{\mathrm{e}_i^j})}{\log(\frac{h^{j+1}}{h^j})}, \quad j = 1, 2, 3 \quad \text{and} \quad i = 1, 2.$$

Finally, the stabilisation terms are selected as

$$S_1^E(\boldsymbol{u}_h, \boldsymbol{v}_h) = 2\mu \sum_{i=1}^{\mathrm{DOF}_1} \mathrm{dof}_i(\boldsymbol{u}_h)\mathrm{dof}_i(\boldsymbol{v}_h), \quad S_2^E(\boldsymbol{\zeta}_h, \boldsymbol{\xi}_h) = \|\int_E \mathbb{M}^{-1}(\boldsymbol{\varepsilon}(w_h), \tilde{r}_h)\|_F \sum_{i=1}^{\mathrm{DOF}_2} \mathrm{dof}_i(\boldsymbol{\zeta}_h)\mathrm{dof}_i(\boldsymbol{\xi}_h).$$

Table 6.1 - 6.2 summarise the convergence history of the mixed VEM (4.20), and we observe the convergence rate of order $O(h^{k_1})$ and $O(h^{k_2+1})$ as predicted in Theorem 5.2. Finally, we present a snapshot of the approximated solutions in the deformed configuration given by $\boldsymbol{u}_h$ for the components of the total flux $\zeta_h = (\boldsymbol{\zeta}_{1,h}, \boldsymbol{\zeta}_{2,h})$, the Herrmann pressure $\tilde{p}_h$ and the concentration φ_h (see Figure 6.3).

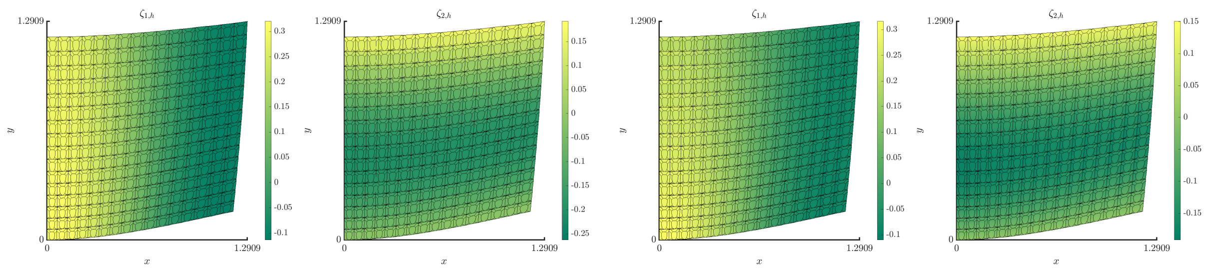

(a) total flux components for $k_1 = 2$ and $k_2 = 0$. (b) total flux components for $k_1 = 2$ and $k_2 = 1$.

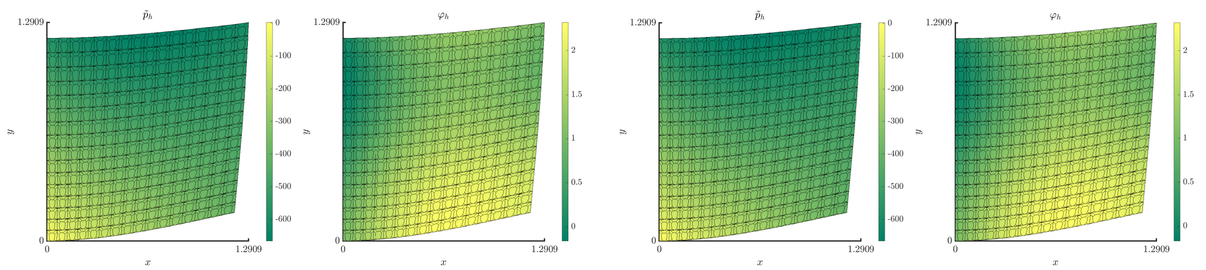

(c) Pressure, concentration for $k_1 = 2$ and $k_2 = 0$. (d) Pressure, concentration for $k_1 = 2$ and $k_2 = 1$.

FIG. 6.3. *Example 1. Snapshot of the approximated solution for the flux $\boldsymbol{\zeta}_h = (\zeta_{1,h}, \zeta_{2,h})^{\mathrm{t}}$, Herrmann pressure $\tilde{p}_h$, and concentration φ_h in the deformed configuration $\boldsymbol{u}_h$ are shown over a "kangaroo face" mesh with 2560 elements for $k_1 = 2$ and $k_2 = 0, 1$.*

6.2. Example 2: Robustness test for a variation in the physical parameters. In this example, we consider a non–convex mesh with a successive refinement of 64, 144, 256 and 400 elements (see (a) Figure 6.1), and expand upon the example introduced in Subsection 6.1 by introducing variations in the physical parameters λ, μ and θ (see Figure 6.4). Test 1 and Test 2 specifically investigate the dependency of the parameter M on λ and μ. As expected, it is observed that this dependency has no impact on the convergence rates. On the other hand, Test 3 shows that M remains independent of a variation in θ and the convergence rates are preserved under the condition $0 \leq \theta < \frac{1}{M} \leq 1$.

We recall that the parameters that remain constant throughout the analysis are held fixed with the values outlined in Subsection 6.1. In light of this, it is important to note that the conditions $1 \leq \lambda$, $0 < \mu$, and $0 < \theta \leq \frac{1}{M} \leq 1$ are satisfied for each test. As predicted in Theorem 5.2, Figure 6.4 shows that the variation of the physical parameters λ, μ, and θ does not affect the expected convergence rates.

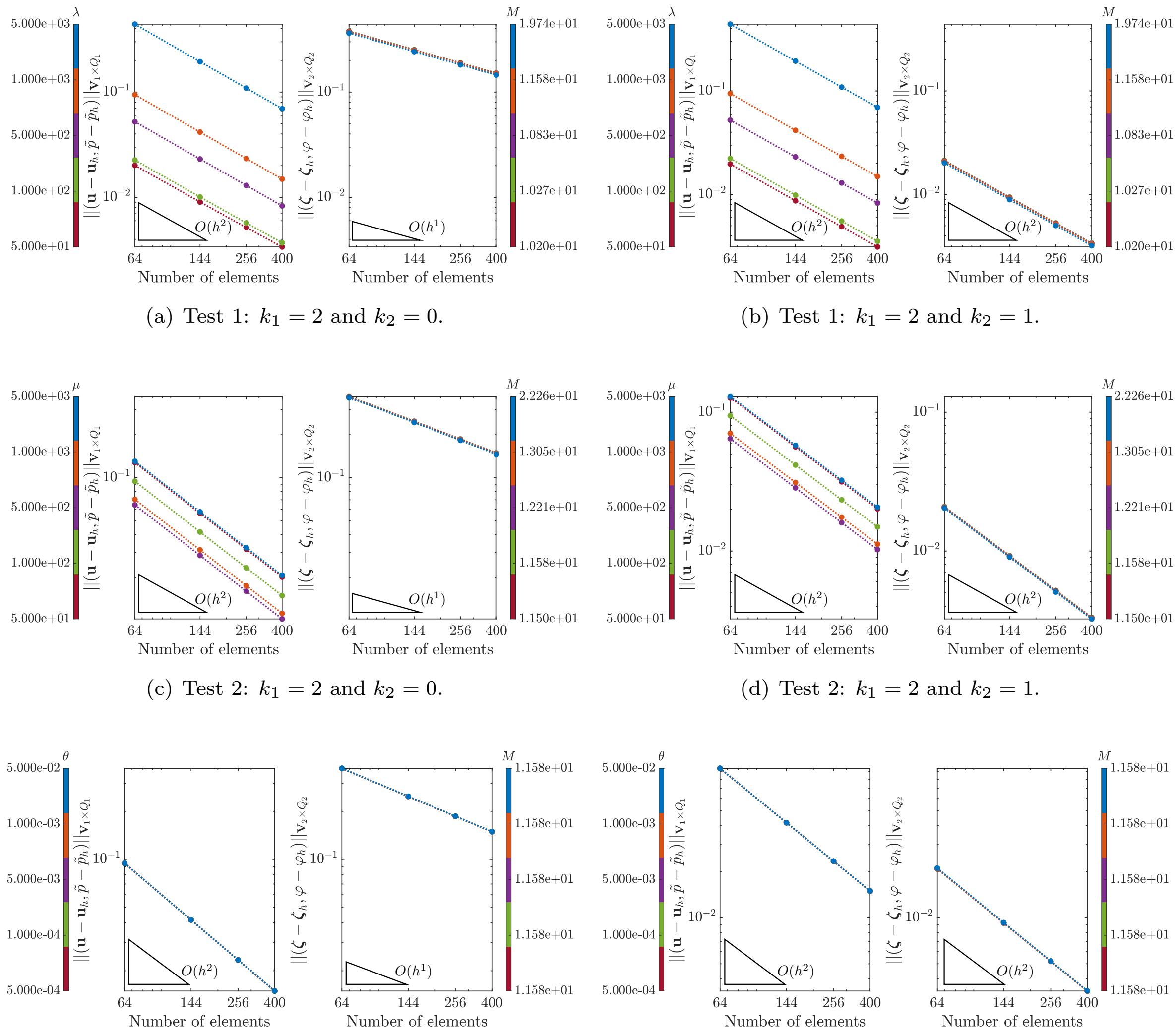

(a) Test 1: $k_1 = 2$ and $k_2 = 0$.

(b) Test 1: $k_1 = 2$ and $k_2 = 1$.

(c) Test 2: $k_1 = 2$ and $k_2 = 0$.

(d) Test 2: $k_1 = 2$ and $k_2 = 1$.

(e) Test 3: $k_1 = 2$ and $k_2 = 0$.

(f) Test 3: $k_1 = 2$ and $k_2 = 1$.

FIG. 6.4. *Example 2. Error history for $k_1 = 2$ and $k_2 = 0, 1$ is illustrated by examining the impact of varying the physical parameters λ, μ, and θ (first, second, and third row). The accompanying side color bars indicate the values of the parameter variation.*

6.3. Example 3: Lithiation of an anode. In this example, we investigate the 2D version of the model presented in [33], and simulate the microscopic lithiation of a perforated circular anode particle (see Figure 6.5)). The outer and inner radius of the particle are $\rho_o = 5$ and $\rho_i = 1$, respectively. We discretise the domain with a Voronoi mesh of 10000 elements and the VE spaces are selected as in Section 4 with $k_1 = 2$ and $k_2 = 1$. In this test, the particle is clamped on the inner circumference Γ_i, a constant current density of $2_{\overline{2}}$ is imposed on the outer circumference Γ_o and zero lithium fluxes are prescribed on Γ_i. The maximum lithium concentration $\hat{\Omega} = 3.497d - 6^{3}_{-}$ is fixed on Γ_o. We check two cases: zero traction and a traction of 1 in the inner normal direction on Γ_o. The Young's modulus is given by $E = 10$ and the Poisson ratio is $\nu = 0.3$, and from these values, we compute $\lambda = \frac{E\nu}{(1+\nu)(1-2\nu)}$ and $\mu = \frac{E}{2(1+\nu)}$. The diffusive source is zero and there is no body load force. The stress-assisted diffusion coefficient is given by $\mathbb{M}(\boldsymbol{\sigma}) = m_0 \exp(-m_1 \operatorname{tr} \boldsymbol{\sigma})\mathbb{I}$ with $m_0 = 1$, $m_1 = 0$ for the constant case and $m_0 = 1$, $m_1 = 10^{-5}$ for the stress-dependent case. The active stress is measured as follows $\ell(\varphi) = K_0\varphi$, where $K_0 = \tilde{\Omega}\frac{2\mu+3\lambda}{3}$ and the partial molar volume is $\tilde{\Omega} = 3.497d - 6^{\frac{3}{-}}$. Finally, the remaining parameters are set as $\theta = M = 1$.

In Figure 6.6 we can observe how the presence of a stress-dependent coefficient $\mathbb{M}(\boldsymbol{\sigma})$ in each case (no traction and traction applied) has an impact on the behaviour of the concentration along the radial direction of the particle which coincides qualitatively with the simulations reported in [33].

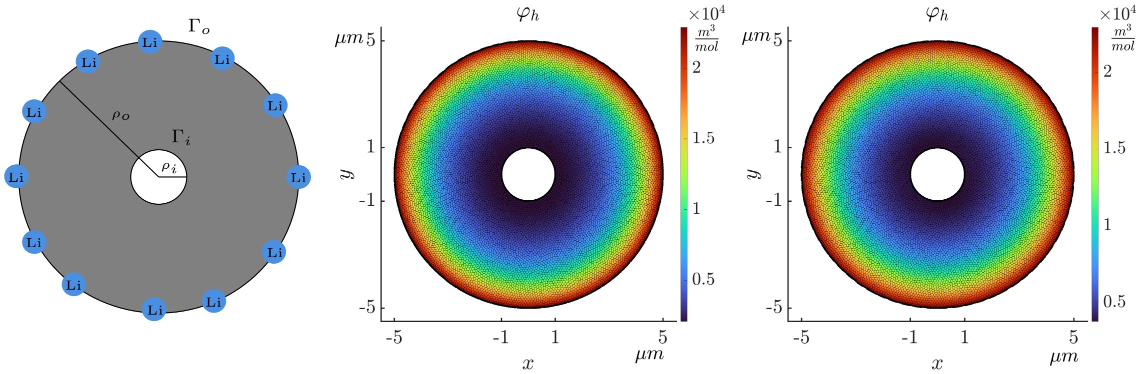

(a) Sketch of a silicon anode. (b) Zero traction. (c) 1 traction.

FIG. 6.5. *Example 3. (left) Perforated circle anode particle with $\rho_i = 1\mu m$ and $\rho_o = 5\mu m$, the maximal Lithium concentration in Γ_o is shown and the particle is clamped on Γ_i. (center and right) solution for non-constant stress-assisted coefficient.*

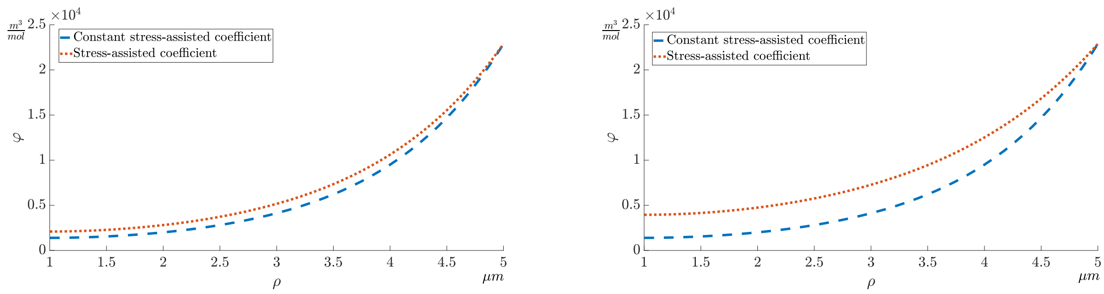

(a) Zero traction. (b) 1 traction.

FIG. 6.6. *Example 3. Concentration φ in the radial direction ρ for a constant and non-constant stress-assisted coefficient.*

Mesh	DOF$_1$	$\mathrm{e}_1(\boldsymbol{u}-\boldsymbol{u}_h, \tilde{p}-\tilde{p}_h)$	r_1	DOF$_2$	$\mathrm{e}_2(\boldsymbol{\zeta}-\boldsymbol{\zeta}_h, \varphi-\varphi_h)$	r_2	iterations
non–convex	1218	9.44e-02	*	320	3.71e-01	*	3
	2738	4.17e-02	2.01	720	2.48e-01	0.99	3
	4866	2.34e-02	2.01	1280	1.86e-01	0.99	3
	7602	1.49e-02	2.00	2000	1.49e-01	0.99	3
Voronoi	962	7.84e-02	*	256	3.61e-01	*	3
	2154	3.47e-02	2.01	574	2.41e-01	0.99	3
	3810	1.97e-02	1.96	1016	1.79e-01	1.02	3
	5994	1.20e-02	2.20	1598	1.44e-01	0.98	3
squares	770	7.92e-02	*	208	3.61e-01	*	3
	1682	3.52e-02	1.99	456	2.41e-01	0.99	3
	2946	1.98e-02	1.99	800	1.81e-01	0.99	3
	4562	1.27e-02	2.00	1240	1.45e-01	0.99	3

TABLE 6.1
Example 1. Convergence history for smooth manufactured solutions, using the polynomial degrees $k_1 = 2$ and $k_2 = 0$.

REFERENCES

Mesh	DOF_1	$\mathrm{e}_1(\boldsymbol{u}-\boldsymbol{u}_h,\tilde{p}-\tilde{p}_h)$	r_1	DOF_2	$\mathrm{e}_2(\boldsymbol{\zeta}-\boldsymbol{\zeta}_h,\varphi-\varphi_h)$	r_2	iterations
non–convex	1218	9.44e-02	*	896	2.09e-02	*	3
	2738	4.17e-02	2.01	2016	9.24e-03	2.00	3
	4866	2.34e-02	2.01	3584	5.19e-03	2.00	3
	7602	1.49e-02	2.00	5600	3.32e-03	2.00	3
Voronoi	962	7.84e-02	*	768	2.03e-02	*	3
	2154	3.46e-02	2.01	1724	9.34e-03	1.91	3
	3810	1.97e-02	1.96	3056	5.37e-03	1.92	3
	5994	1.20e-02	2.20	4796	3.33e-03	2.14	3
squares	770	7.92e-02	*	672	1.89e-02	*	3
	1682	3.52e-02	1.99	1488	8.34e-03	2.02	3
	2946	1.98e-02	2.00	2624	4.67e-03	2.01	3
	4562	1.27e-02	2.00	4080	2.98e-03	2.01	3

TABLE 6.2
Example 1. Convergence history for smooth manufactured solutions, using the polynomial degrees $k_1 = 2$ and $k_2 = 1$.

[1] P. F. Antonietti, G. Vacca, and M. Verani, *Virtual element method for the Navier–Stokes equation coupled with the heat equation*, IMA Journal of Numerical Analysis, 43 (2023), pp. 3396–3429.
[2] L. Beirão da Veiga, F. Brezzi, A. Cangiani, G. Manzini, L. D. Marini, and A. Russo, *Basic principles of virtual element methods*, Mathematical Models and Methods in Applied Sciences, 23 (2013), pp. 199–214.
[3] L. Beirão da Veiga, F. Brezzi, L. D. Marini, and A. Russo, *Mixed virtual element methods for general second order elliptic problems on polygonal meshes*, ESAIM Mathematical Modelling and Numerical Analysis, 50 (2016), pp. 727–747.
[4] L. Beirão da Veiga, C. Lovadina, and G. Vacca, *Divergence free virtual elements for the Stokes problem on polygonal meshes*, ESAIM Mathematical Modelling and Numerical Analysis, 51 (2017), pp. 509–535.
[5] L. Beirão da Veiga, F. Dassi, and G. Vacca, *The stokes complex for virtual elements in three dimensions*, Mathematical Models and Methods in Applied Sciences, 30 (2020), pp. 477–512.
[6] D. Boffi, F. Brezzi, and M. Fortin, *Mixed Finite Element Methods and Applications*, vol. 44, Springer-Verlag, Berlin, 2013.
[7] W. Boon, M. Kuchta, K.-A. Mardal, and R. Ruiz-Baier, *Robust preconditioners and stability analysis for perturbed saddle-point problems – application to conservative discretizations of Biot's equations utilizing total pressure*, SIAM Journal on Scientific Computing, 43 (2021), pp. B961–B983.
[8] D. Braess, *Stability of saddle point problems with penalty*, M2AN - Modélisation mathématique et analyse numérique, 30 (1996), pp. 731–742.
[9] S. C. Brenner and L. R. Scott, *Polynomial Approximation Theory in Sobolev Spaces*, Springer New York, New York, NY, 1994, pp. 91–122.
[10] F. Brezzi, R. S. Falk, and L. Donatella Marini, *Basic principles of mixed virtual element methods*, ESAIM: Mathematical Modelling and Numerical Analysis, 48 (2014), p. 1227–1240.
[11] C. Cherubini, S. Filippi, A. Gizzi, and R. Ruiz-Baier, *A note on stress-driven anisotropic diffusion and its role in active deformable media*, Journal of Theoretical Biology, 430 (2017), pp. 221–228.
[12] F. Dassi, A. Fumagalli, A. Scotti, and G. Vacca, *Bend 3d mixed virtual element method for Darcy problems*, Computers & Mathematics with Applications, 119 (2022), pp. 1–12.
[13] A. Ern and J.-L. Guermond, *Theory and Practice of Finite Elements*, Applied Mathematical Sciences, 159. Springer-Verlag, New York, 2004.
[14] G. N. Gatica, *A Simple Introduction to the Mixed Finite Element Method. Theory and Applications*, Springer-Verlag, Berlin, 2014.
[15] G. N. Gatica, B. Gómez-Vargas, and R. Ruiz-Baier, *Analysis and mixed-primal finite element discretisations for stress-assisted diffusion problems*, Computer Methods in Applied Mechanics and Engineering, 337 (2018), pp. 411–438.
[16] ———, *Formulation and analysis of fully-mixed finite element methods for stress-assisted diffusion problems*, Computers & Mathematics with Applications, 77 (2019), pp. 1312–1330.
[17] ———, *A posteriori error analysis of mixed finite element methods for stress-assisted diffusion problems*, Journal of Computational and Applied Mathematics, 409 (2022), p. 114144.
[18] G. N. Gatica, C. Inzunza, and F. A. Sequeira, *A pseudostress-based mixed-primal finite element method for stress-assisted diffusion problems in Banach spaces*, Journal of Scientific Computing, 92 (2022), pp. Paper No. 103, 43.
[19] B. Gómez-Vargas, K.-A. Mardal, R. Ruiz-Baier, and V. Vinje, *Twofold saddle-point formulation of Biot poroelasticity with stress-dependent diffusion*, SIAM Journal on Numerical Analysis, 63 (2023), pp. 1449–1481.
[20] P. Grigoreva, E. N. Vilchevskaya, and W. H. Müller, *Stress and Diffusion Assisted Chemical Reaction Front Kinetics in Cylindrical Structures*, Springer International Publishing, Cham, 2019, pp. 53–72.
[21] L. Herrmann, *Elasticity equations for incompressible and nearly incompressible materials by a variational theorem*, AIAA Journal, 3 (1965), pp. 1896–1900.
[22] A. Khan, C. E. Powell, and D. J. Silvester, *Robust a posteriori error estimators for mixed approximation of nearly incompressible elasticity*, International Journal for Numerical Methods in Engineering, 119 (2019), pp. 18–37.
[23] S. Kumar, R. Oyarzúa, R. Ruiz-Baier, and R. Sandilya, *Conservative discontinuous finite volume and mixed schemes for a new four-field formulation in poroelasticity*, ESAIM: Mathematical Modelling and Numerical Analysis, 54 (2020), pp. 273–299.
[24] T. Kuroki, T. Ito, and K. Onishi, *Boundary element method in Biot's linear consolidation*, Applied Mathematical

Modelling, 6 (1982), pp. 105–110.
[25] M. Lewicka and P. B. Mucha, *A local and global well-posedness results for the general stress-assisted diffusion systems*, Journal of Elasticity, 123 (2016), pp. 19–41.
[26] H. Malaeke and M. Asghari, *A mathematical formulation for analysis of diffusion-induced stresses in micropolar elastic solids*, Archive of Applied Mechanics, 93 (2023), pp. 3093–3111.
[27] J. Martins, E. Pires, R. Salvado, and P. Dinis, *A numerical model of passive and active behavior of skeletal muscles*, Computer Methods in Applied Mechanics and Engineering, 151 (1998), pp. 419–433.
[28] J. Meng, L. Beirão da Veiga, and L. Mascotto, *Stability and interpolation properties for stokes-like virtual element spaces*, Journal of Scientific Computing, 94 (2023), p. e56.
[29] J. D. Murray and J. D. Murray, *Mathematical Biology: II: Spatial Models and Biomedical Applications*, vol. 3, Springer, 2003.
[30] J. D. Murray and G. F. Oster, *Generation of biological pattern and form*, Mathematical Medicine and Biology: A Journal of the IMA, 1 (1984), pp. 51–75.
[31] M. A. Olshanskii, J. Peters, and A. Reusken, *Uniform preconditioners for a parameter dependent saddle point problem with application to generalized Stokes interface equations*, Numerische Mathematik, 105 (2006), pp. 159–191.
[32] O. J. Sutton, *The virtual element method in 50 lines of MATLAB*, Numerical Algorithms, 75 (2017), pp. 1141–1159.
[33] M. Taralov, *Simulation of Degradation Processes in Lithium-Ion Batteries*, doctoralthesis, Technische Universität Kaiserslautern, 2015.
[34] D. Unger and E. Aifantis, *On the theory of stress-assisted diffusion, II*, Acta Mechanica, 47 (1983), pp. 117–151.
[35] R. Wilson and E. Aifantis, *On the theory of stress-assisted diffusion, I*, Acta Mechanica, 45 (1982), pp. 273–296.
[36] Y. Yu, *mVEM: A MATLAB software package for the virtual element methods*, arXiv preprint, 2204.01339 (2022).
[37] T. Zohdi and P. Wriggers, *On the effects of microstress on macroscopic diffusion processes*, Acta Mechanica, 136 (1999), pp. 91–107.